Università di Foggia

HR EXCELLENCE IN RESEARCH

PhD Programme in

"TRANSLATIONAL MEDICINE AND MANAGEMENT OF HEALTH SYSTEM - XXXIV CYCLE"

PhD Director: prof.ssa Teresa Santantonio

The pivotal role of Inflammaging in the peritumoral tissue of Renal Cell Carcinoma: from potential regulating mechanisms to clinical significance

Supervisor

Prof. Giuseppe Grandaliano

GIUSEPPE GRANDALIANO
20.06.2023 12:44:38
GMT+01:00

Advisor

Prof.ssa Elena RANIERI

PhD Student

dott.ssa Federica SPADACCINO

2018-2021

Sono rotti i miei legami
pagati i miei debiti
le mie porte spalancate
me ne vado da ogni parte.
Essi accovacciati nel loro angolo
continuano a tessere
la pallida tela delle loro ore;
o tornano a sedersi nella polvere
a contare le loro monete
e mi chiamano, e mi chiamano
perché torni indietro
Ma già la mia spada è forgiata,
già ho messo l'armatura
già il mio cavallo è impaziente
e io guadagnerò il mio Regno.

"Carmen '63"
da Tagore

INDEX

ABSTRACT

Chronic, low-grade inflammation and cell senescence, also named Inflammaging, impacts tumor progression via the secretion of senescence-associated secretory phenotype (SASP). Here, we explored the role of inflammaging in the context of Renal Cell Carcinoma (RCC).

The expression of pro-inflammatory (PTX3) and SASP-related proteins (p21/ CIP1/WAF1, p16/INK4a, IL-6) in the peritumoral (periRCC) and tumoral (RCC) area of renal samples from 10 patients undergone radical nephrectomy for RCC was evaluated by confocal microscopy. Moreover, an *in vitro* analysis on normal renal proximal tubular epithelial cells (RPTECs) under hypoxia conditions and in RCC cell lines was conducted by western blotting and qPCR.

An increased expression of PTX3 and IL-6 in both periRCC and RCC tissues, as compared to normal renal tissues ($p<0.001$) was observed, while an increased expression of p21 and p16 levels from normal to periRCC ($p <0.001$) and their reduction in RCC tissues ($p <0.05$) was also observed.

The *in vitro* analysis showed that under conditions of 1% hypoxia, expression of PTX3 and IL-6 was significantly and progressively increased in RPTEC and RCC cell lines in a time-dependent manner. Interestingly, expression of p21 and p16 were upregulated in hypoxic RPTEC while in RCC cell lines, p21 was similarly expressed to RPTEC at baseline and p16 expression was undetectable.

In the context of molecular mechanisms, a coordinate increase in the gene expression of PTX3 and miR-224-5p over time under hypoxic conditions in normal and in ccRCC cells and tissues was observed. Furthermore,

classifying tissues according to Fuhrman Grading, operational differences in the senescence status of peritumoral vs. tumor core RCC tissues were detected. Higher levels of PTX3 and IL-6 and lower level of cell cycle inhibitors in high grade (G3-G4) than in low-grade tumors (G1-G2), both in periRCC and RCC tissues, were observed. This study paves the way to an improved understanding of inflammaging as a mechanism impacting ccRCC disease progression. The downregulation of cell cycle inhibitors and the increased expression of pro-inflammatory factors appear to be crucial for tumor progression and clinical significance of the disease.

1. INTRODUCTION

1.1 RENAL CELL CARCINOMA

Renal cell carcinoma (RCC) is the most widespread type of renal neoplasia and it accounts for about 3-4% of cancer diagnoses in adults in western countries [1]. RCC incidence is higher in males and in more economically developed countries with frequencies increasing at a rate of 2-4% per year and consequent increases noted in mortality (equal to 2.2 cases / 100,000 inhabitants) which mainly affects the 55-65 years old age group [2,3]. RCC is considered an enigmatic tumor as only 10% of patients manifest the classic triad of clinical symptoms consisting of severe haematuria, pain and palpable flank mass. More than 60% of RCC patients, rather, show an asymptomatic clinical course and, for this reason, diagnosis of most RCC cases is often accidental, following diagnostic tests performed for other clinical conditions [4].

The main risk factors contributing to the development of RCC are advanced age, obesity, hypertension, smoking and the presence of concomitant or pre-existing kidney diseases, however, hereditary forms linked to genetic factors are also common [5].

Furthermore, RCC is a chemo- and radio-resistant neoplasia, therefore the current therapeutic strategies prioritize surgical approaches (radical and/or partial nephrectomy, or tumorectomy) [6].

However, these strategies are very invasive. The 5-year patients' survival rate after surgery is estimated to be around 70-80% for those with localized

cancer, while it is less than 10% for patients with metastatic forms [6]. The significant difference in the survival rate of patients with metastases, as compared with those without, stresses the urgency to identify new diagnostic models and biomarkers allowing for improvement in the early detection of RCC. In recent years, the discovery of mechanisms underlying the pathogenesis of RCC has been crucial for testing and introducing new protocols based on targeted therapy approaches into clinical practice, including the administration of anti-angiogenic agents, mTOR inhibitors and immune checkpoint inhibitors [7].

1.1.1 PATHOGENESIS OF THE RENAL CELL CARCINOMA

RCC encompasses a heterogeneous group of neoplasms resulting from the malignant transformation of the kidney's tubular epithelial cells. The most common form of cancer accounting for 90% of all cases is represented by the adenocarcinoma, typically in the unilateral form [8,9,10]. Three histotypes of RCC can be distinguished: clear cell (ccRCC), papillary (pRCC) and chromophobe (chRCC) [11]. ccRCC is the most frequently diagnosed form: it is found in over 70% of all cases of RCC and, due to its natural metastatic tendency, is also the most clinically severe [12]. Cases of ccRCC are characterized by the presence of abundant lipid and glycogen cytoplasmic deposits giving the kidney a yellowish colour visible even under macroscopic observation, leading to attribution of the “clear cell” definition (**Figure 1**) [13].

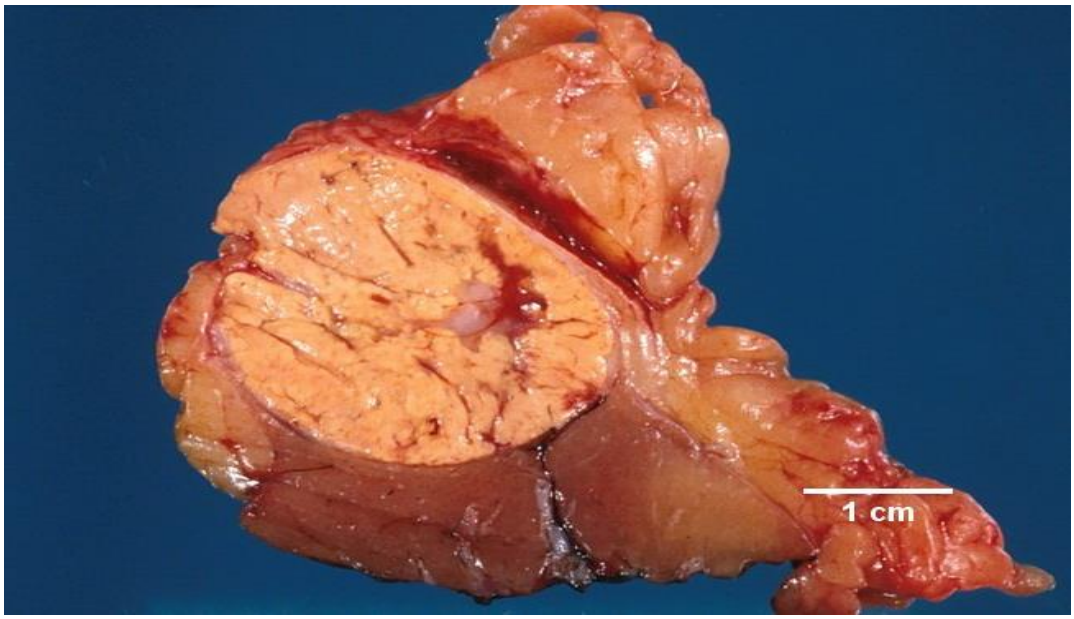

Figure 1. Macroscopic appearance of clear cell renal carcinoma.
Clear cell renal carcinoma sample from a partial nephrectomy. The tumor is well circumscribed and shows the classic yellow-gold appearance due to lipid deposits**.**

The ccRCC can be sporadic (> 96%) or familial (<4%) [14]. The mutation of the von Hippel-Lindau tumor suppressor gene (VHL), located on chromosome 3 (locus 3p25) has been found in numerous cases of ccRCC, indicating a close correlation with the onset of the neoplasm. Patients with this syndrome show renal cysts and multiple bilateral ccRCCs [15].

The VHL gene encodes the pVHL protein which acts as a substrate for the ubiquitin protein-ligase complex with polyubiquitination function and targets a range of proteins, including HIF-1 (hypoxia induced factor-1). HIF-1 is a heterodimer composed of an α and a β subunit; under normoxic conditions HIF-1α is produced and regulated at the post-translational level through a hydroxylation reaction on two highly conserved proline residues (P402 and P564), by prolyl-hydroxylase (PHD) and HIF prolyl-hydroxylase (HPH) enzymes which use oxygen as the main reaction substrate. Following

the hydroxylation of proline, HIF-1α binds pVHL and degradation of HIF-1α is mediated by the proteasome. On the other hand, under conditions of hypoxia or when mutations occur in genes encoding relevant processing enzymes, the degradation of HIF-1 mediated by pVHL is interrupted. Consequently, the α-subunit of HIF-1 associates with the β-subunit and the resulting heterodimeric complex translocates into the nucleus, where it binds DNA sequences containing Hypoxia Responsive Elements (HRE) in their gene promoter regions, resulting in the transcription of downstream genes associated with cell survival. Some of the genes capable of counteracting hypoxia regulated by HIF include VEGF, PDGF, TGF-β, EGFR, EPO and CAIX [16].

In ccRCC, genetic inactivation due to mutations in the VHL gene results in the stabilization of HIF-1α protein even under normoxic conditions, leading to induced expression of genes including *VEGF, PDGF, TGF-β, EGFR, IGF, GLUC1, EPO, CXCR4*. These downstream target genes play a fundamental role in the pathogenesis of ccRCC by altering cell metabolism, inducing angiogenesis and promoting metastatic invasion and growth. Genetic alterations in the VHL gene also promote stabilization of HIF-2. The activation of HIF-1 and HIF-2 is closely related, with both factors activating genes containing HRE sequences in their promoter regions under hypoxic conditions. Structurally, HIF-1 and HIF-2 are very similar in that they share 48% amino-acid sequence identity and have a high degree of homology in their oxygen-dependent domains [17]. It has been reported that about 40% of ccRCC tumors contain HIF-1 locus deletions and exhibit only HIF-2 activation. Therefore, mutated VHL tumors can be classified according to

their differential expression of HIF factors; i.e., H1H2 vs H2 tumors [18-19]. In fact, numerous studies have shown that differential inactivation of HIF-1 and HIF-2 leads to the development of altered phenotypes, probably due to the activation of different intrinsic transcriptional programming in tumor cells [20].

Several researchers have shown that HIF-2 plays a protumor role by enhancing expression of the proto-oncoprotein MYC, a transcription factor that promotes cell proliferation and protein synthesis and is highly expressed in more than 40% of human tumors. On the other hand, HIF-1α appears to act as an oncosuppressor, inhibiting expression of the MYC protein [21]. Moreover, the presence of deletions in the chromosome 14q region, where the HIF-1α gene is located, appear related to reduced survival in patients with metastatic ccRCC, with tumors expressing only HIF-2 being characterised by higher rates of cell proliferation than those expressing both HIF-1 and HIF-2 [22].

1.2 THE ROLE OF INFLAMMATION IN THE EVOLVING RCC TUMOR MICROENVIRONMENT

The tumor microenvironment (TME) is considered a highly heterogeneous and dynamic network involving interactions between different cell components and the extracellular matrix that are conditioned by intrinsic tumor factors, some of which are secreted to mediate localized field effects [23]. In this way, cancer cells may act: 1) directly by releasing certain growth factors or cytokines; 2) indirectly by inducing a state of hypoxia; or 3) by

elaborating chemoattractants for other cell types that facilitate disease progression.

In recent years, numerous studies have attempted to identify conditions predisposing the host to development of ccRCC, and cancer in general. In this context, the study of evolving conditions in the TME appear critical to understanding disease pathogenesis and to identify key pathways for targeted antagonism in the therapeutic setting [24].

During oncogenesis, inflammation (i.e., reactive immunoflogosis) serves as an acute process to counteract the development of neoplastic cells. On the other hand, it is well known that chronic inflammation may paradoxically favor the progression of neoplasms, in part by enriching the TME with pro-inflammatory cytokines and growth factors that induce an uncontrolled proliferative response [25-26].

1.3 PENTRAXINS

Within the chronic inflammatory context predisposing to development of neoplasia, pentraxins have been increasingly recognized for their modulatory role in this process. Pentraxin 3 (PTX3) is an opsonin belonging to the superfamily of fluid-phase pattern recognition molecules (PRMs) impacting innate elements of the immune system [27].

Pentraxins have been divided into two groups: short or “classical” pentraxins and long pentraxins, which differ in their structure, chromosomal localization, gene expression, cellular source and ligands. C-reactive protein (CRP) and serum amyloid P component (SAP) represent members of the short pentraxin sub-family and are characterized by the

distinctive pentraxin structural signature, a primary motif of eight amino acids (His-x-Cys-x-Ser/Thr-Trp-x-Ser, where x is any amino acid) in the protein's carboxy-terminal region [28].

On the other hand, Neuronal pentraxin 1 (NPTX1), neuronal pentraxin 2 (NPTX2), pentraxin 3 (PTX3) and pentraxin 4 (PTX4) are long pentraxin family members that contain an extra and somewhat peculiar amino-terminal domain which is responsible for the protein's binding activities [29].

The similarity of PTX3 with C-reactive protein (CRP), the most commonly recognized inflammatory biomarker in the clinical setting, has led to intense investigation of the role of PTX3 in a range of infectious disease states and inflammatory disorders.

1.3.1 ROLE OF PTX3 IN INFLAMMATION

PTX3 is prototypical of long pentraxins and exerts a multifunctional role impacting resistance to pathogens, opsonisation via Fc receptor, clearance of apoptotic cells, inflammation and even fertility [30]. The human PTX3 gene is encoded on chromosome 3q25 and consists of three exons, coding respectively for the leader peptide, the N-terminal domain and the pentraxin domain, with these exon domain separated by two introns [27].

Unlike the short pentraxins that are synthesized primarily by the liver and systemically released in the blood, PTX3 is synthesized by several types of cells and tissues, most notably by macrophages and dendritic cells of the immune system, as well as by endothelial, mesenchymal and epithelial cells (including kidney epithelial cells). PTX3 is constitutively stored in

neutrophil-specific granules in a ready-made bioactive form. PTX3 is rapidly released within sites of tissue damage or infection in response to inflammatory signals such as Tumor Necrosis Factor-α (TNF-α) and Interleukin-1β (IL-1β), where it plays an important role in the early phases of inflammation. It serves as a peripheral index of inflammation, with plasma levels of PTX3 promptly increasing from baseline values of 2 ng/ml to up to 200–800 ng/ml within 6 to 8 hours after the occurrence of an inflammatory event [31,32,33,34,35]. Of interest, PTX3 can also be found in other body fluids, including urine, cerebrospinal, pleural, amniotic and joint fluid [36].

1.3.2 PTX3: FROM INFLAMMATION TO CARCINOGENESIS

Inflammatory cytokines and growth factors progressively create a cellular and biochemical microenvironment characterized by a state of chronic, low-grade inflammation in which PTX3 seems to be a peculiar player. PTX3 appears intimately involved in carcinogenesis based on its ability to affect the pathogenesis of different cancers and by exerting a dualistic role in relation to the neoplastic type, cellular source and the TME (**Figure 2**) [31, 37]: it can act as oncogene by promoting tumor cell proliferation, migration/invasion, pro-tumor macrophage chemotaxis and tumor escape from immunosurveillance or as a tumor suppressor by inducing dysregulation of pro-tumor mitogenic pathways, and by inhibiting angiogenesis, metastatic potential of tumor cells, as well as epithelial-to-mesenchymal transition (EMT) [37,38]. During the process of tumorigenesis, immunoflogosis represents an acute process that prevents

the development of cancer. In this context, the resolution of inflammation in the TME is rare and, as previously reported, chronic inflammation strongly impacts cancer progression [39]. PTX3 has a pivotal role in tumor initiation and exerts a pro-tumorigenic role by interacting with the PI3K/AKT/mTOR signalling pathway to enforce tumor cell proliferation and metastasis as well as, the processes of EMT and drug resistance in several types of neoplasia [40,41,42,43].

Based on its pro-tumor function, PTX3 is considered an unfavorable prognostic factor for basal-like breast cancers, female reproductive system tumors, lung, gastric and pancreatic cancers, glioma, liposarcoma, melanoma and prostate cancer [37, 44, 45].

Having said this, the role of PTX3 in cancer development is pleiotropic and likely to be context dependent, since in some cases PTX3 expression may result in suppression of tumor initiation and be correlated to extended patient overall survival (OS) [37]. Indeed, in several cancer types the binding of PTX3 to selected members of the fibroblast growth factor family (FGF), including FGF2, and FGF8b through its N-terminal domain, inhibits FGF-dependent tumor neovascularization, EMT and metastatic spread [47, 48, 49].

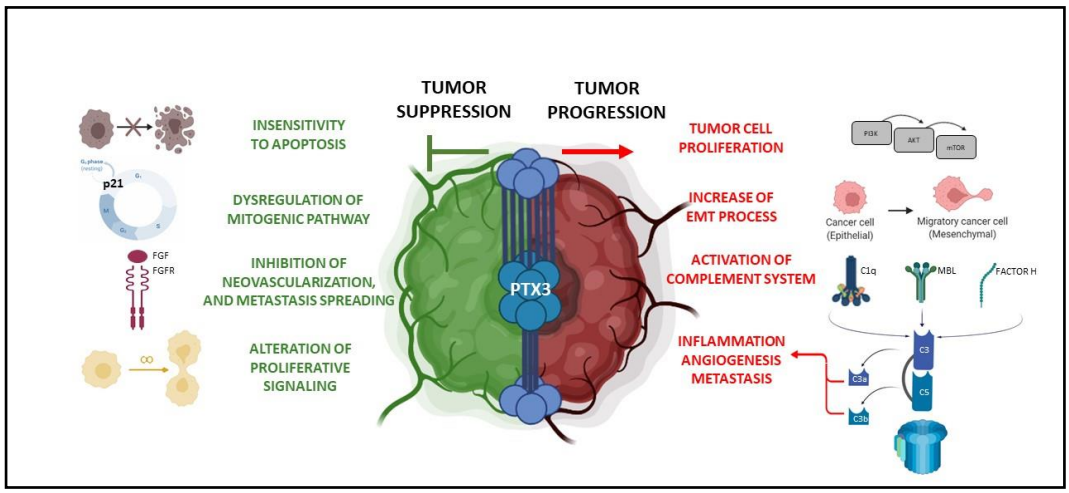

Figure 2: The complex role of PTX3 in cancer development and progression.
The role of PTX3 in cancer pathogenesis is likely to be context dependent. PTX3 acts as oncogene via PI3K/AKT/mTOR pathway by inducing cell proliferation, metastasis spreading, EMT processes, tumor cell migration/invasion and drug resistance. On the contrary, in some cases PTX3 may act as a tumor suppressor factor by inducing insensitivity to apoptosis and by promoting cell-cycle arrest.

PTX3 also plays a complex role in complement system (CS) modulation, since the effect of CS activation or inhibition depends on the type of ligand bound and on the inflammatory and tumor context in which such binding occurs [46, 50]. Noteworthy, PTX3 shares with the other short classic pentraxins the ability to directly interact with the key molecules involved in the activation and/or regulation of CS cascade. Indeed, PTX3 induces the activation of the classical pathway and the lectin pathway by binding to C1q and MBL, resulting in regulation of the alternative pathway via CFH binding. Activation of the classical and lectin pathways may be mediated by the antibody-like common features of the pentraxins, leading to the recruitment of C1 complex and MBL to the membrane-attachment complex (MAC) formation [30,51,52]. In addition, by binding to complement regulators, such as C4BP and CFH, PTX3 fails to promote chronic

inflammation-dependent damage to the host by mediating resolution of inflammatory processes [53].

Complement factors are mainly synthesized in the liver, but both tumor and stromal cells within the TME share the ability to produce complement proteins [54]. As part of the innate immune system, CS enhances the ability of antibodies and phagocytic cells to promote inflammation. Regardless of the involved pathway, the activation of CS culminates with C3 and C5 cleavage by C3 and C5 convertase, respectively, up to the membrane attack complex (MAC) formation (i.e., C5b-9 complex) to mediate lysis of neoplastic cells and/or cellular pathogens. Of note, in the TME, complement mediators coordinately induce anti-tumor responses mainly via their lytic activity and enriching the environment with immunosuppressive factors that promote carcinogenesis by releasing strong pro-inflammatory molecules (i.e. C3a, C5a) that sustain neoangiogenesis and tumor metastasis. Indeed, cells that express receptors for C3a and C5a including leucocytes, endothelial, epithelial cells, fibroblasts and macrophages induce pro-inflammatory interleukin release [55]. Furthermore, C3a and C5a promote activation of the PI3K/Akt/mTOR pathway which is strongly associated with neoplasia [56,57,58]. Conversely, in the attempt to evade immune recognition/control, cancer cells may upregulate expression of membrane bound Complement Regulatory Proteins (mCRPs), including CD55, CD59, CD46 that serve as CS inhibitors [59].

1.3.3 PTX3 IN GENITOURINARY TUMORS

PTX3 plays a particularly significant role in genitourinary cancers.

In pilot work, our research group demonstrated that PTX3 serum levels clearly discriminate patients with benign prostatic hyperplasia (BPH) from those with prostate cancer (PC). In addition, PTX3 tissue expression levels may also identify those patients with chronic inflammation at the time of initial prostate biopsy who are at higher risk to develop PC [60]. In this study, the lack of correlation between serum levels of PTX3 and CRP allowed us to rule out the possibility that elevated levels of PTX3 simply resulted from systemic inflammation. PC patients are known to express high levels of prostate-specific antigen (PSA), a serine protease capable of cleave/activating C3 and C5 in vitro [61]. Notably, elevated levels of C3 fragments are found in the serum of PC patients [61, 62] and an increase in expression of CD55 and CD59 has been observed in patients with advanced PC in association with decreased OS [62, 63].

Furthermore, in a subsequent study we showed that PTX3 expression is quantitatively, temporarily and spatially correlated with expression of C1q, but not MBL, and hence it appears to be involved in the development of PC via the sustained activation of the classical pathway. Moreover, in our studies, we observed that the production of CD59 (aka protectin), that is ubiquitously expressed at low levels under normal conditions, was significantly increased in the patients who subsequently developed PC at the time of first and second biopsy [64].

The inflammatory milieu in the TME of RCC is likely further amplified since renal cells are capable of secreting all of the complement effector molecules triggering the classical pathway [65, 66].

Indeed, elevated levels of C5a and expression of CD55/CD59 and CD46 in ccRCC patients represents an adverse prognostic feature [67, 68, 69, 70]. In another study, our research team showed that PTX3 influences the ccRCC TME and represents a local/systemic marker of cancer-related inflammation. More specifically, we observed that PTX3 is not only remarkably expressed in the ccRCC cells and RCC tissues when compared to normal cells/tissues, but that its expression is related to the modulation of CS.

Interestingly, expression of PTX3 co-localizes with that of C1q, C3aR, C5aR and CD59 deposition, but not with the C5b-9 complex, supporting the hypothesis that the pro-tumorigenic effects of both CS and PTX3 sustain neoangiogenesis in the absence of neoplastic cell cytolysis [71]. In addition, we retrospectively validated expression of PTX3 as reliably biomarker in the ccRCC setting since we observed that PTX3 serum levels at the time of diagnosis were remarkably elevated in a large cohort of RCC patients vs. healthy donors. In a follow-up study, we observed a reduction in PTX3 levels in patients undergoing interventional surgery. Furthermore, we observed that at time of diagnosis, significantly higher serum levels of PTX3 occurred in patients with higher Fuhrman grade, lymph node involvement and visceral metastases.

These data support the contention that PTX3 serum levels are significantly associated with ccRCC-specific 10 year OS, thus defining PTX3 as

potentially useful biomarker for the diagnosis and prognosis of patients with ccRCC [71].

1.4 MicroRNAs: biogenesis and function

The analysis of microRNAs (miRNAs), small non-coding endogenous RNAs, is relevant given the pleiotropic roles that they play in oncology. MiRNAs regulate gene expression at both the transcriptional and post-transcriptional levels, by binding to complementary sequences present in target messenger RNA (mRNA) molecules. Productive miRNA/mRNA interactions lead to repression in target mRNA translation or preferential degradation of the targeted protein molecule by proteasomes [72].

The biogenesis of miRNAs involves a series of steps occurring in the cell nucleus/cytoplasm whereby a long-stranded double-stranded RNA is progressively converted into a single-stranded effector miRNA. In the nucleus, RNA polymerase II transcribes a long primary strand, up to 10kb in length, called a primary miRNA (pri-miRNA). This transcription is followed by three steps: i.) *cropping*, in which the microprocessor protein complex, consisting of RNA polymerase III, Drosha and Pasha/DGCR8, cleaves the pri-miRNA into a precursor miRNA (pre-miRNA) to form a hairpin structure, defined hairpin-loop, of 70 bases with hydroxyl group at the 3' end and a phosphate group at the 5' end; ii.) *export* in which the pre-miRNA, by binding the Esportin 5 protein, is transported into the cytoplasm; and iii.) *dicing* in which the pre-miRNA is processed by dicer cytoplasmic RNA polymerase III into a mature duplex miRNA of about 22-25 nucleotides in length (**Figure 3**) [73, 74, 75].

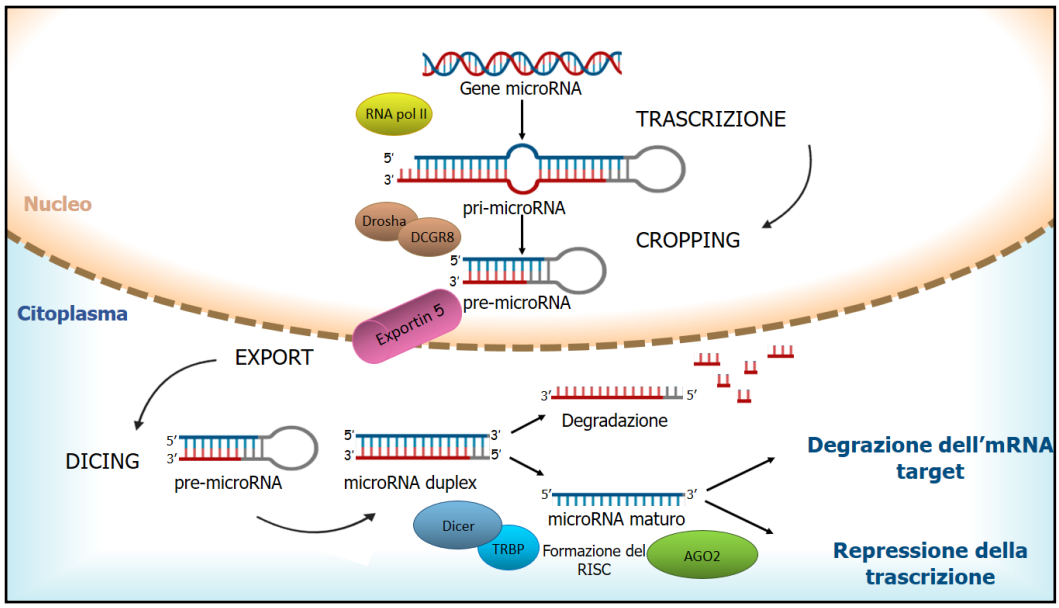

Figure 3. Biogenesis of miRNAs
The synthesis of primary miRNA (pri-miRNA) by RNA polymerase II occurs in the nucleus. The subsequent maturation involves three steps: *cropping*, in which the pri-miRNA is processed by the microprocessor complex to form a hairpin structure called precursor miRNA (pre-miRNA); *export*, in which the pre-miRNA by binding exportin 5, is transported into the cytoplasm and *dicing* that leads to the generation of mature duplex miRNA.
Mature miRNA binds to TRBP and AGO 2 proteins to form the RNA-induced silencing complex (RISC) inducing post-transcriptional regulation. (Modified from: Spadaccino F, et al. Pharmaceuticals 2021, 14, 322).

By binding to Argonaute proteins (AGO), the miRNA duplex is incorporated into the RNA-induced silencing complex (RISC), where the interaction between the miRNA and the target mRNA takes place [76]. However, only one of the two strands that form the miRNA duplex is retained and directed to the regulation of target proteins. The other strand, called the passenger strand, is expelled from the complex and degraded. It has been reported that the orientation of the hairpin directs the fate of the two filaments. Indeed, depending on whether the filament deriving from the 3' or the 5' arm is incorporated (i.e. miRNA-3p and miRNA-5p), different target molecule profiles are developed [77].

RISC binds the 3' UTR region of the target mRNA and depending on the complementarity of that interaction, target transcript degradation or blocking of translation occurs.

The net biological function of a given miRNA depends on range of target mRNAs that it recognizes. In fact, the same miRNA may bind different target RNAs, just as a given target RNA can be the target of several unrelated miRNAs.

miRNAs influence a broad range of biological processes such as tissue differentiation, cell growth, cell proliferation and apoptosis. Furthermore, miRNAs are subjected to fine regulation and any mutation that affects one or more enzymes of the miRNA maturation process may lead to disease-associated gene dysregulation. Such dysregulation can play a crucial role in the progression of various diseases, including cancer [78]. It is now known that over 60% of human protein coding genes have miRNA target sites in their 3' UTR region and, therefore, their associated protein expression may be strictly regulated by miRNAs under both normal and pathologic conditions [78].

1.4.1 THE onco-miRNAs

Cancer cells have a high proliferative capacity with the ability to evade the immune response and intrinsic cellular apoptosis, while promoting the processes of angiogenesis, tissue invasion and metastasis. Tumorigenesis has classically been considered a consequence of the deregulated expression of oncogenes and/or loss of tumor suppressors, due to gene mutations or epigenetic modifications. However, miRNAs also appear to be involved. In

tumor tissues, oncogenic miRNAs (oncomiRs) are commonly over-expressed and are hypothesized to be associated with dysregulated expression of tumor suppressor gene products. It has been reported that the miR-17-92 cluster acts as an oncogene by mitigating mechanisms of apoptosis and thereby inhibiting cell death. On the other hand, low intrinsic expression of tumor suppressor miRNAs (TS-miR) can induce the overexpression of target molecules directly associated with tumor growth. Common TS-miRNAs include miR-34a, miR-15a, miR-16-1 and miR-let-7 [79, 80, 81].

Activation or inactivation of miRNAs results in the under- or over-expression of target genes/proteins, respectively. Ultimately it is the function performed by the endpoint target transcripts/proteins that determines whether a miRNA should be considered as an oncogene or a tumor suppressor.

1.4.2 MiRNAs IN RENAL CELL CARCINOMA

Several studies have highlighted the involvement of miRNAs in RCC tumorigenesis. In particular, miR-17-5p, miR-224 and miR-210 have been reported to contribute to progressive tumor growth by positively impacting the HIF-1α pathway. There is also a strong inverse correlation between miR-92 and the expression of VHL in different subtypes of RCC. Overexpression of this miRNA could affect HIF-1 transcription independent of VHL mutation and thus regulate RCC progression [82]. Other reports have suggested that the miRNA-200 family is involved in several events that favor development of RCC. In particular, an inverse correlation was

observed between VEGF levels and expression of some members of the miRNA-200 family, demonstrating that the loss of these miRNAs is involved in reinforced angiogenesis in RCC tumors [83, 84].

Furthermore, tumor suppressor miRNAs miR-126, miR-378, miR-100 and oncogenic miRNA miR-200b promote angiogenesis while miR-122, miR-153-5p and miR-205-5p contribute positively to tumor proliferation by targeting components of the PI3K/Akt/mTOR pathway [85].

1.5 CELL SENESCENCE

Within the context of the TME, recent studies have highlighted a pivotal role played by the process of cellular senescence. Senescence is a mechanism of cellular adaptation that induces permanent cell-cycle arrest. Physiologically, senescence can be activated in response to intrinsic and extrinsic stimuli such as shortening or structural changes of telomeres, mitogenic signals, activation of oncogenes, epigenetic alterations, mitochondrial dysfunction, inflammation as well as, the introduction of chemotherapy agents [86, 87]. Senescence is considered a highly dynamic process in which cells evolve progressively and in a context-specific manner, accompanied by phenotypic alterations such as chromatin remodelling, metabolic reprogramming and increased autophagy [88].

Senescence was originally considered as a process that occurred only in cell culture, but recently it has been shown to play a fundamental role in physiological processes such as tissue repair, cell homeostasis maintenance, regulation of hormone secretion, and pathological processes such as cancer, atherosclerosis, diabetes, and many others [89, 90].

Senescence is activated as a result of the ageing process in association with the development of age-related diseases or conditionally upon treatment with chemotherapeutic drugs [91].

Cell senescence is different from other forms of cell cycle arrest, like quiescence, as it arrests cells in the G1 phase of cell-cycle, while quiescence directs cells into the G0 phase. Moreover, one characteristic of quiescent cells is the possibility of resuming proliferation in response to specific signals, such as growth factors, an event that does not occur during senescence [92, 93].

Senescent cells are characterised by increased lysosomal activity, macromolecular and morphological damage both resulting in the acquisition of a vacuolized and enlarged form, defined as "flattened" [94, 95, 96]. Senescence is a multi-step process. In the first phase called "early senescence", the cells enter in the state of cell cycle arrest due to negative regulatory signals. Then the cells undergo a progressive remodelling of chromatin resulting in the release of factors necessary for the maintenance of senescence, yielding the so-called "full-senescence" phase. If senescent cells persist in this state for an extended time, they continue to evolve through various phenotypes, ultimately reaching the “late senescence” phase [97]. In addition, it should be noted that two types of *in vivo* senescence can be distinguished: acute senescence, which is a condition generated in response to mild cell stress that helps restore tissue homeostasis [98]; and chronic senescence that emerges as a consequence of prolonged alterations, such as a chronic inflammatory state or oncogenic activation ("oncogene induced senescence" OIS). These processes involve

the release of pro-inflammatory factors including cytokines, chemokines and growth factors [99].

1.5.1 REGULATION OF SENESCENCE

The cell cycle arrest pathways play a fundamental role in the regulation of senescence. Retinoblastoma (Rb) protein, the key nuclear phosphoprotein of cell cycle regulation, binds to the E2F protein, keeping it in its inactive state thereby blocking cells in the G1 phase. Phosphorylation levels of the Rb protein are known to be cell cycle-dependent [100]. Hypophosphorylated forms prevail in the phases of quiescence or terminal differentiation, while more phosphorylated forms occur from the late G1 phase up to the M cell cycle phase [101]. During the G1 phase, D cyclins bind to CDK4-6 and the resulting molecular complex phosphorylates serine and threonine residues in the Rb protein resulting in reduced affinity for its substrate. The E2F protein, when no longer bound to the Rb protein, activates and induces the transcription of genes involved in cell cycle progression [102].

Among cell cycle suppressors it is worth mentioning the p53 protein, also called the «guardian of the genome», which in case of DNA mutations or alterations, induces cell cycle arrest. In greater detail, protein p53 promotes the *de novo* synthesis of $p21^{CIP1/WAF1}$ protein belonging to the Cip/Kip protein family, together with p27 and p57 proteins [103]. The p21 protein is a cyclin-dependent kinase inhibitor (CDKI) that blocks the Cyclin D/CDK4-6 complex, thereby inhibiting the release of E2F by the Rb protein. Under conditions of severe DNA damage, p53 may activate mechanisms that

prevent neoplastic transformation such as apoptosis. Due to its key tumor suppressor role, a mutation in the P53 gene has been identified in ~50% of all human tumors [104]. Another class of CDKI is the family of INK4/ARF proteins. This family includes the tumor suppressor $p16^{INK4a}$ which induces the slowing of G1 phase and the S phase transition by inhibiting phosphorylation of the Rb protein by CDK4-6 [105]. Alterations in p16 protein have been found in numerous neoplastic cell types [106].

During cell cycle arrest, the p53 tumor suppressor, once activated, regulates an antiproliferative transcriptional program up to p21 transcription [107]. If the stress that triggers the senescence process is transient, p53 can direct the cell into a quiescent state, allowing the cell to repair DNA damage. Persistent stress, on the other hand, activates p16, thus inducing a condition of terminal senescence [108]. P21 shows a divergent role in the progression of the cell cycle depending on its level of expression. High p21 levels inhibit the cyclin D/CDK4-6 complex by inducing cell cycle arrest; on the contrary, low levels of p21 induce complex assembly and promotion of cell cycle progression [109, 110]. Furthermore, p21 promotes senescence in every phase of the cell cycle unlike p16 which only acts during the G0/G1 cell cycle phase. Notably, "loss of function" mutations in p16 are among the most commonly detected somatic gene alterations in human tumors. Senescent tumor cells are found in many cancers at the pre-invasive stage, but this is no longer the case for invasive (advanced) tumors. For this reason, p16 is considered one of the most specific markers of (tumor) cell senescence *in vivo* [95].

1.5.2 SENESCENCE-ASSOCIATED SECRETORY PHENOTYPE (SASP)

By retaining metabolic activity, senescent cells remain competent to release inflammatory factors that can affect the surrounding tissue microenvironment/TME (**Figure 4**) [95]. The resulting phenotype is called Senescence-Associated Secretory Phenotype (SASP), with elaborated mediators including proinflammatory cytokines, chemokines, growth factors, angiogenetic factors, proteases, extracellular matrix components and metalloproteinases [111, 112]. The secretome associated with SASP varies according to the type of cell, the stimulus that induces senescence and the duration of the senescence process. SASP factors may be produced in the form of soluble proteins directly secreted into the surrounding environment, or as transmembrane molecules that undergo shedding via proteolytic release from the cell surface [111]. SASP factors are responsible for the cancer-related effects associated with senescent cells. Among soluble factors, the most prominent SASP cytokine is interleukin (IL)-6, a pleiotropic pro-inflammatory cytokine whose secretion is strikingly increased after DNA damage- and oncogene-induced senescence in several cell types. [112, 113]. Most senescent human cells also overexpress IL-8 and IL-1α [112, 114]. IL-6 and IL-8 expression depends on production and release of IL-1α, which then acts as a feed-forward inducer and regulator of SASP. Of note, IL-6 and IL-8 secreted by senescent fibroblasts promotes EMT in several neoplasms [115, 116, 117]. Among SASP-associated elaborated growth factors, the insulin-like growth factor (IGF)/IGFR pathway may also contribute to the impact of senescent endothelial,

epithelial and fibroblast cells in the TME. Also, colony stimulating factors (CSFs including granulocyte-macrophage (GM)-CSF and granulocyte (G)-CSF) are secreted at high levels by senescent fibroblasts [112]. Moreover, amphiregulin and VEGF are growth factors found to be upregulated in senescent fibroblasts [118, 119]. In addition to these soluble factors, senescent cells also secrete increased levels of matrix metalloproteinases (MMPs) including stromelysin-1 and -2 (respectively, MMP-3 and -10) and collagenase-1 (MMP-1) which may also modulate the bioactivity of SASP soluble factors [120, 121, 122]. Furthermore, senescent cells may secrete non-proteinaceous molecules, including reactive oxygen species (ROS) that promote cancer cell aggressiveness/invasiveness [123].

Remarkably, SASP factors may also induce cellular senescence in neighbouring cells which is primarily mediated by TGF-β family members and VEGF [124]. In particular, IL-6 can facilitate cellular reprogramming by inducing the expression of stem cell markers in neighbouring cells leading to a state of de-differentation, which contributes to cancer therapy resistance. [125, 126, 127]. The effect of SASP autocrine and paracrine signalling in neoplastic transformation is therefore contextual and pleiotropic [112]. While some studies claim that SASP protects cells from pathological conditions, others consider this paradigm to enforce a state of neoplastic transformation [95].

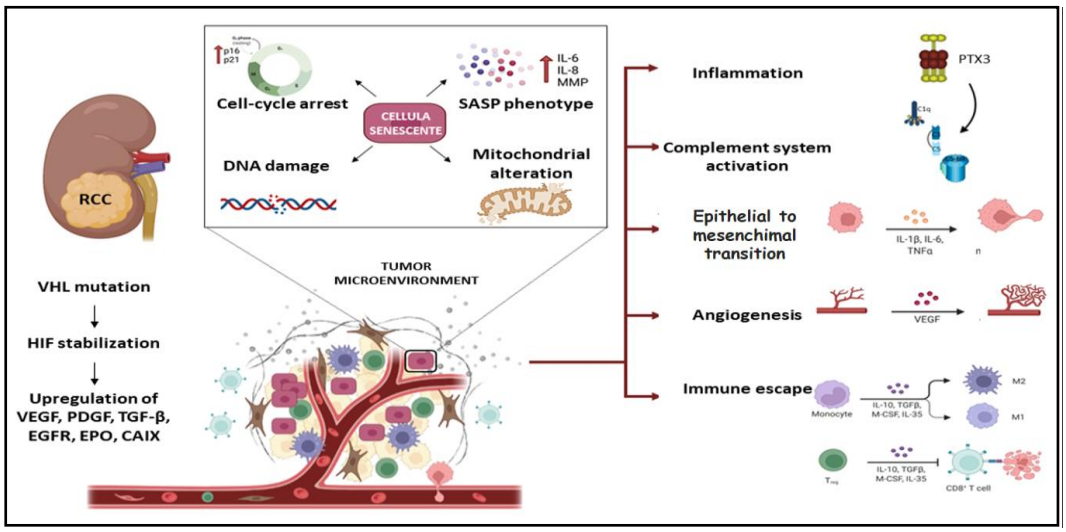

Figure 4. The TME of ccRCC
The ccRCC TME is highly-heterogeneous and composed of diverse cell populations embedded within a hypoxic extracellular matrix in which senescent cells appear to play equivocal roles, by counteracting neoplastic proliferation via cell cycle arrest and by releasing cytokines that support tumor progression by sustaining a state of chronic inflammation.

1.5.3 SENESCENCE IN RENAL CELL CARCINOMA

How senescence may affect the TME of ccRCC remains poorly studied. Within the tumor milieu, the accumulation of SASP molecules promotes inflammation while regulating anti-tumor immunity [128].

Recent studies have shown that activation of senescence is a hallmark of ccRCC. Although in ccRCC the most frequent mutation involves the VHL gene, other mutations involving genes encoding by 3p fragments are not uncommon (e.g., PBRM1, BAP1, and SETD2) [1291]. Indeed, the senescence process has been closely linked to genomic instability and an imbalance in PBMR1/BAP1 mutations in ccRCC [130].

In addition, aging/senescence-induced genes (ASIGs) are known to be upregulated in malignant diseases [131]. In this context, a novel prognostic

model of eight ASIGs, including FOXG1, FOXM1, GNRH1, HAMP, IGFBP2, IL10, MPEG1, and VASH1, showed significant value in predicting survival in ccRCC patients [132].

Several mechanisms underlying renal cell/RCC senescence have been discovered.

Autophagy is a highly conserved survival mechanism, a process that helps cells to “self-eat” endogenous material and recycle cellular components to maintain cellular integrity and energy which is essential to maintaining kidney homeostasis, structure and function. In the acute injury phase of acute kidney injury (AKI), autophagy is induced in proximal tubules and acts as a protective mechanism that is crucial for tissue repair during the recovery phase. Dysregulation of autophagy is associated with an accumulation of autophagosomes, intracellular damaged proteins, and organelles that contribute to the progressive deterioration of kidney function [133].

Loss of Klotho expression modulates aging–associated pathways.

Klotho is a transmembrane anti-aging protein that is strongly expressed in the kidney where it inhibits interstitial fibrosis, accumulation of cell cycle-arrested cells, increased levels of oxidative stress and TGF-β1-related signaling pathways [134].

Impaired mitochondrial oxidative phosphorylation is associated with both aging and cellular senescence in humans. Several studies have demonstrated that both acute and chronic insults lead to alterations in mitochondrial structure, membrane integrity and mitochondrial DNA (mtDNA) damage [135].

Epigenetic modifications are stable, heritable, and reversible genome changes that occur without altering genomic DNA sequences and which are important in healthy and accelerated renal aging.

Several studies investigating the role of senescence in kidneys suggest that cellular senescence is responsible for the pathogenesis associated with diverse forms of kidney diseases including diabetic nephropathy, acute and chronic kidney disease, ischemia/reperfusion injury (IRI), glomerular diseases and renal transplantation graft rejection, but little is known about senescence as it relates to the evolution of ccRCC [136, 137, 138, 139].

2. AIM OF THE STUDY

Inflammation and senescence are processes with contextual implications in cancer progression. Based on the latest evidence and literature, the scientific community has recently coined the term "*Inflammaging*" to define the state of systemic, low grade, chronic inflammation status associated with the process of senescence.

To date, little is known about the role of inflammaging in the progression of RCC and the molecular mechanisms underlying this disease-associated process.

The aim of this study was to:

- identify and evaluate the effect of miRNAs on PTX3 modulation in ccRCC cells and tissues;
- elucidate the direct involvement of the miRNA identified on tumor cell expression of PTX3 and SASP, via functional transfection analyses.
- assess the correlation between PTX3 expression and the SASP phenotype (p21CIP1/WAF1, p16INK4a, IL-6) in the tumor and peritumoral regions of clinical specimens isolated from patients undergoing radical nephrectomy for RCC;
- analyse the expression of PTX3 and SASP-related proteins in both proximal tubule (RPTEC) renal cells and RCC cell lines.

3. MATERIALS AND METHODS

3.1 BIOLOGICAL SAMPLES

Cell lines

The cell samples analysed were derived from primary and immortalized cell lines. In detail, primary renal tumor lines derived from ccRCC tissue isolates and a well-characterized, established ccRCC cell line (RCCBA85#21) were used in these studies. A primary line of renal proximal tubular epithelial cells (RPTEC) was employed as a control. Primary RCC cells were cultured in complete medium (AR5), consisting of Roswell Park Memorial Institute medium (RPMI) (Sigma Aldrich, Saint Louis) supplemented with Fetal Bovine Serum 20% (FBS), L-Glutamine 1%, Penicillin/Streptomycin 1%, growth factors and stabilizers such as Insulin 20 ug/ml, Apo-Transferrin 10 ug/mL, Na selenite 25 nM, Hidrocortisone 50 nM, EGF 0,001 ug/ml Ethanolamine 10 uM, Phosphorylethanolamine 10 uM, Triiodothyronine (T3) 100 pM, Hepes 10 Mm and Na pyruvate 5 mM. RCCBA85 and RPTEC cells were cultured in RPMI and in Dulbecco's modified Eagle's medium (DMEM)–F12 medium (ThermoFisher), respectively. These media were supplemented with 10% fetal bovine serum (FBS), 2 mM l-glutamine, and 100 U/ml penicillin–streptomycin (all from Sigma-Aldrich). Where indicated, RPTECs were exposed to 1% hypoxia and cultured for 8, 24 and 48 hours prior to analysis.

Study population and tissue collection

Samples of pathological, peritumoral and tumor tissue were collected from 10 primary ccRCC tumors after patient nephrectomy at the Urology and

Kidney Transplantation Center of the Polyclinic “Riuniti” of Foggia. A control group of 10 subjects who underwent renal biopsy in the Nephrology Unit of the Polyclinic “Riuniti” of Foggia for suspected chronic nephropathy, but whose tissues exhibited a normal renal histology were also analyzed. Two pathologists confirmed the presence of ccRCC in the neoplastic tissues and the exclusion of tumor cells in healthy specimens. Tumor and normal tissues were collected, formalin-fixed and paraffin-embedded (FFPE sample) according to standard procedures and stored at room temperature until time of analysis. The 2016 World Health Organization and Fuhrman classifications were used to attribute histological type and nuclear grade, respectively. Written informed consent to take part in the study was given by all participants.

3.2 PROTEIN LYSIS

To obtain protein extracts, cells were lysed into RIPA lysis buffer + 1% of protease inhibitors by cell scraping. The cell lysate was centrifuged at 12,000 g for 15 minutes and then stored at -80°C. Protein titration was carried out by indirect quantification using the Bradford method (Bio-rad protein assay) at a wavelength of 595 nm.

3.3 WESTERN BLOTTING

Immunoblotting was used to evaluate expression of protein markers of interest (PTX3, IL-6, p21, p16). Protein samples were analysed by SDS-PAGE under denaturing conditions. Samples were denatured with Laemmli sample buffer 4x (62.5 mm Tris-HCl, pH 6.8, 10% glycerol, 0.005%

Bromophenol Blue), + 10% β-mercaptoethanol for 8 minutes at 90 °C. The run was carried out on polyacrylamide gel with concentration gradient from 4 to 15 % (Mini-protean TGX stain-free). In each gel, wells were loaded with 30 ug of total protein. The run was performed in 10x Tris/Glycine/SDS buffer at 150 V for 5 minutes and 200 V for 25 minutes. For the electroblotting, a membrane of polyvinylidene fluoride (PVDF mini format 0.2 μm) and Trans-Blot Turbo for 3 minutes at 25 volts were used. Membranes were subsequently incubated in a blocking buffer (BSA 5% in PBS-Tween 0,05 %) and then incubated at 4°C o.n. with the following primary antibodies: anti-PTX3 1:1000; anti-IL-6 1:1000; anti-p21 1:2000; anti-p16 1:500. All antibodies were diluted in PBS-Tween 0.05% + BSA 1%. After washing 3 times for 10 minutes each in 0.05% PBS-Tween 0,05%, the following secondary antibodies were applied: goat anti-mouse HRP antibody (ab6789, Abcam, Cambridge UK) diluted 1:10000; goat anti-rabbit HRP antibody (ab97051, Abcam, Cambridge UK) diluted 1:20000; goat anti-rat HRP antibody (ab6734) diluted 1:2500. All antibodies were diluted in PBS-Tween 0.05%. For detection, Clarity western substrate (Biorad) was used. In addition, to allow for normalization of the results, all membranes were incubated with the primary anti-β-actin antibody (AHP2417) diluted 1:40000.

3.4 ISOLATION OF CELLS FROM RCC TISSUES

The portions of renal pathological and normal tissues, collected in the operating room under sterile conditions, were fragmented using a scalpel blade into 1 mm^3 pieces. The tissue fragments were then subjected to

enzymatic digestion for 15 minutes at RT usinga solution of collagenase IV (10%), hyaluronidase (1%) and DNase (0.2%) in Hanks' Balanced Salt Solution (HBSS) (Thermo Fisher Scientific, Waltham, MA, USA). The tissue fragments were repeatedly transferred through metal sieves of 200 μm and 180 μm of mesh, and the filtrate of cells collected. After centrifugation at 1500 rpm for 10 minutes, the cell pellet was resuspended in complete RCC cell medium (AR5).

The resuspended cells were plated in a 25 cm^2 flask and incubated at 37 ° C and 5% CO2. After 2-3 days, the culture medium was changed, eliminating cellular debris and non-adherent cells, with plastic adherent tumor cell lines expanded and maintained in CM.

3.5 RNA EXTRACTION

For the extraction of RNA from cells and tissues, the RNeasy MiniKit (74104, Qiagen, Hilden) and miRNeasy (217004, Qiagen, Hilden) kits were used. Cell lysis was initially carried out using TRIzol + β-mercaptoethanol for the extraction of total RNA and QIAzol for the extraction of miRNAs only. TRIzol and QIAzol consist of a blend of guanidine histothiocyanate, an RNase and DNase inhibitor and denaturant, and phenol, a water insoluble organic denaturant. The addition of chloroform allowed the separation of the mixture into three distinct phases: an organic phase on the bottom containing DNA, proteins and lipids, a separation interface and a surface aqueous phase containing RNA. The RNA was precipitated by ethanol on the filter of a column and subsequently subjected to subsequent washing and purification phases by buffering and centrifugation at high speeds.

Finally, the RNA was eluted in RNase-free water and quantitated (NanoDrop 1000 Spectrophotometer, Thermo Fisher).

3.6 GENE EXPRESSION ANALYSES

To quantify the expression levels of specific RNAs, Real-time PCR and Retro-Transcriptional PCR (RT-PCR) were performed. The following probes were used: miR-224-5p (Hs_miRNA-224-5pAssay ID CTYMJTG, Thermo Fisher Scientific, Waltham, MA, USA) PTX3 (Hs01073991_m1, Thermo Fisher Scientific, Waltham, MA, USA).

The extracted RNA was first converted into complementary DNA by RT-PCR (High-capacity reverse transcription kit, Applied Biosystems) and subsequently amplified by Real-time PCR (Applied Biosystems, Foster City) using specific primer pairs. Data were normalized against a constitutive control gene: RNU6B (U6 _Assay ID 001093, Thermo Fisher Scientific, Waltham) for the miRNAs assay and 18S (Hs99999901_s1, Thermo Fisher Scientific, Waltham) for the mRNA assay.

3.7 TRANSFECTION ASSAYS

To confirm the data obtained in RCC cells, a transfection analysis with the mimic and the inhibitor of miR-224-5p in RPTEC cells was conducted. The following probes were used for transfection: MISSION microRNA Mimic hsa-miR-224 and MISSION Synthetic microRNA Inhibitor, hsa-miR-224 (Sigma Aldrich, Saint Louis). The Invitrogen Lipofectamine 2000 (Thermo Fisher Scientific, Waltham, MA) kit was used for transfection.

The analysis required several preliminary tests to establish optimal transfection conditions.

RPTEC cells were plated in 24-well Petri dishes and cultured for 24h in DMEM/F12 with the addition of 5% of FBS without antibiotics, according to kit instructions. The probe/lipid complex was diluted in pure DMEM/F12 medium, without serum, under the following conditions: three conditions with probe concentration of 20 pmol with 0.5-1-1.5 µl of lipid and three conditions with probe concentration equal to 40 pmol with 0.5-1-1.5 µl of lipid.

When the cells reached 30-50% confluence, the probe/lipid complex was added to the plates. The cells were incubated at 37 ° C with 5% CO2 for 5 hours to allow the entry of the complex across the cell membrane. Subsequently, the medium containing the lipid residues, known to be toxic to cells upon extended culture, was eliminated and normal growth medium was added to allow the cells to reach the 70-80% confluence.

The success of the transfection protocol was validated by qPCR. RPTEC cells were transfected with the mimic/lipid complex (20 pmol/1µl) and mimic + inhibitor/lipid (20 pmol + 20 pmol /1µl) and cultured for 48h at 37 ° C with 5% CO2.

3.8 SA-β-Gal TEST

Senescence-associated SA-β-gal staining was performed using a kit per the manufacturer's protocol (Cell Signalling Technology). After washing with PBS (pH 6.0), frozen tissues were fixed in 4% paraformaldehyde for 15 minutes and stained with freshly prepared SA-β –gal solution (1 mg/mL X-

gal, 40 mM citric acid/sodium phosphate (pH 6.0), 5 mM potassium ferrocyanide, 5 mM potassium ferricyanide, 150 mM NaCl, and 2 mM MgCl). Next, tissues were incubated at 37 °C overnight in a dry incubator. The development of blue color was assessed. Nuclei were counterstained with Mayer Hematoxylin.

3.9 INDIRECT IMMUNOFLUORESCENCE ANALYSIS OF RENAL CELLS AND FFPE SPECIMENS

For the purpose of this research project, indirect immunofluorescence (IFI) microscopy was performed on renal cells and paraffin-embedded sections of peritumoral and tumor regions of RCC tissues and normal renal tissue controls.

To perform the IFI on cell lines, it was necessary to culture the cells on suitable supports, called chamber-slides (NalgeNunc International, Naperville, IL, USA), which guarantee cell growth with excellent adherence. Cold methanol was used for 5 minutes for the fixation of the adherent cells in the chamber slides. After washing with PBS pH 7.4, a solution of Triton X- 100 diluted to 0.25% in PBS for 7 minutes was added. Subsequently, cells were incubated for 1 hour in a blocking solution (BSA 2% + FBS 5% in PBS). The following antibodies were the used to stain slides: rabbit monoclonal anti-carbonic anhydrase IX (CAIX) (Ventana Medical System, AZ, USA) at a concentration of 0.14 ug/mL, rabbit monoclonal anti-cytokeratin 7 (CK7) (Ventana Medical System, AZ, USA) at a concentration of 0.536 ug/mL, rat monoclonal anti-PTX3 (Enzo, Villeurbanne, France) diluted 1:100. The following secondary Abs were used: Alexa-Fluor goat anti-rabbit IgG 488

and goat anti-rat IgG 488. All secondary antibodies were diluted in PBS at a ratio of 1:250.

For tissues, the slides were placed in Xylene overnight and then treated in a decreasing concentration of alcohol solutions from 100% to 50%. Subsequently, the sections were hydrated in distilled H2O and then subjected to antigenic exposure by brief microwave treatment in a sodium citrate solution (pH 6). After washing 3 times for 5' each in PBS pH 7.4 and permeabilization in Triton X-100 0,25% (Sigma-Aldrich, Saint Louis, MO, USA) for 8 minutes, histological slides were incubated for 1 hour in a blocking solution (BSA 2% + FBS 0,05% in PBS) and subsequently incubated at 4°C overnight. The following primary antibodies were used for the incubation: rat polyclonal anti-PTX3 antibody (ALX-210-365, Abcam, Cambridge, UK) diluted 1:100; rabbit monoclonal anti-IL-6 antibody (ab6672, Abcam, Cambridge, UK) diluted 1:100; rabbit monoclonal anti-p21 antibody (ab109520, Abcam, Cambridge, UK) diluted 1:500; mouse monoclonal IgG2a anti-p16 antibody (SC-1661 Santa Cruz, Dallas, TX, USA) diluted 1:100; rabbit monoclonal anti-HIF-1α antibody (ab 179483, Abcam, Cambridge, UK) diluted 1:500; mouse monoclonal IgG1 anti-HIF-2α antibody (NB100-132, Novus Biologicals Ltd, Englewood, CO, USA) diluted 1:200. All antibodies were diluted in blocking solution.

After washing in PBS tissue sections and the negative control were incubated 1h at room temperature with the secondary antibodies.

The following secondary antibody (Alexa, Thermo Fisher, Walthan, MA, USA) were used for antigen detection: Alexa-Fluor goat anti-rat IgG 488, goat anti-rabbit IgG 546, goat anti-mouse IgG2a and IgG1 555, goat anti-

mouse IgG2a 488. All secondary antibodies were diluted in PBS at a ratio of 1:250.

To stain the nuclei cells and tissues, samples were incubated with TO-PRO diluted 1:3000 in PBS pH 7,4 (Invitrogen-Molecular Probe, Thermo Fisher, Waltham, MA, USA). The slides were mounted in Gel Mount (Sigma-Aldrich, Saint Louis, MO, USA) and sealed. Specific fluorescence was evaluated by confocal microscopy using the Leica TCS SP5 (Leica, Wetzlar, Germany) equipped with argon-krypton (488 nm) and helium-neon (633 nm) lasers.

3.11 STATISTICS

Statistical analysis was performed using SPSS 17.0 software (SPSS Inc, Evanston, IL). Variable distribution was tested using Kolmogorov-Smirnov test. Different parameters were compared between groups by Student's t-test for unpaired data and Mann-Whitney U-test, as appropriate. Frequencies were compared among groups by X^2-test. All the data were reported as mean ± standard deviation (SD) or as percentage frequency, unless otherwise specified. A p-value <0.05 was considered statistically significant.

4. RESULTS

4.1 ANALYSIS OF MOLECULAR MECHANISMS INVOLVED IN RCC-ASSOCIATED INFLAMMAGING

4.1.1 CHARACTERIZATION OF PRIMARY RCC CELL LINES

Primary RCC cells were isolated from neoplastic tissues by enzymatic digestion and mechanical dissociation through metal sieves, with subsequent expansion in culture to establish primary cell lines (**Figure 5**).

A B

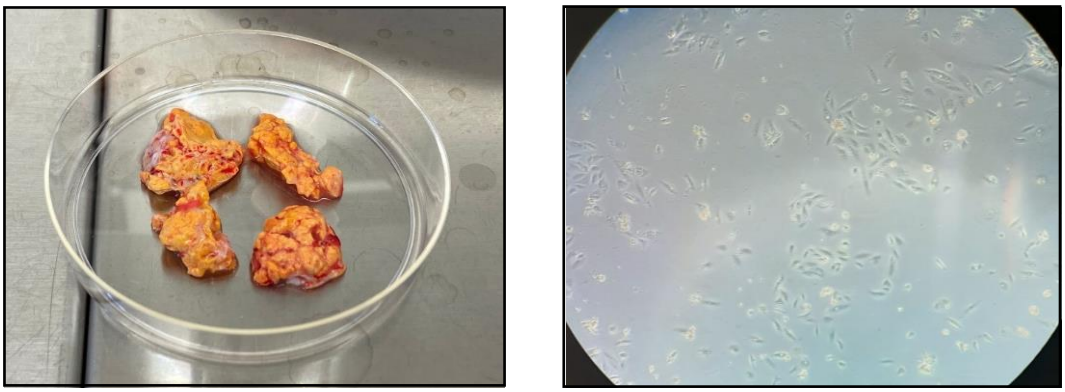

Figure 5: **Isolation and expansion of a primary ccRCC tumor cell lines**
CcRCC tissue harvested by radical nephrectomy exhibits a typically yellow appearance (A). After enzymatic digestion and culture of single cell suspensions in AR5 medium at 37 ° C 5% CO2, adherent primary tumor lines were obtained for subsequent analysis (B).

At the second step, the cells were trypsinized and plated in the chamber-slides for characterization by confocal immunofluorescence microscopy (IFM). Although there are no specific phenotypic markers for ccRCC lines, the positivity of primary RCC cells to antibodies against the CK7 and CAIX antigens allowed us to confirm the epithelial origin and neoplastic characteristics of the isolated tumor cell lines, respectively. (**Figure 6**).

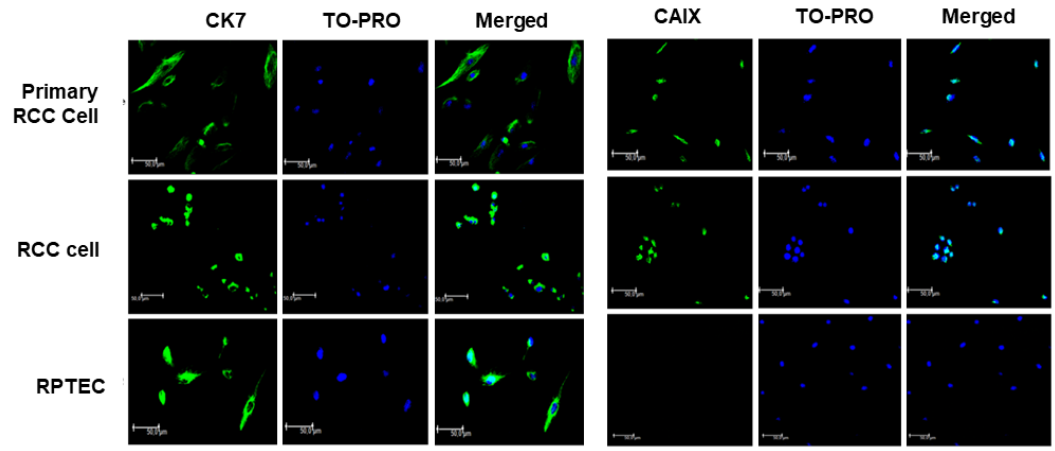

Figure 6: Characterization of primary cells isolated from RCC tissues by immunofluorescence microscopy (IFM)
IFM analysis of primary tumor cell lines revealed positive staining using antibodies directed against the CK7 and CAIX antigens. CK7 is expressed by primary lines isolated from RCC tissue, RCC lines and normal RPTEC cells (A-C, G-I). CAIX is expressed by primary lines and RCC lines while it is absent in normal RPTEC cells (I-L, P-R). Nuclei are stained with TO-PRO-3 (blue).

4.1.2 PTX3 AND miR-224-5p GENE EXPRESSION IN RCC CELLS AND TISSUES

In silico analysis using bioinformatics tools (MiRBase, MiRDB, miRmap) and published studies identified miR-224-5p as the miRNA most likely associated with modulated PTX3 expression in RCC. To confirm this hypothesis, we conducted gene expression profiling of cell lines under normoxic vs. hypoxic conditions using quantitative qRT-PCR. We observed an increase in miR-224-5p expression over time under hypoxic conditions in normal RPTEC (**Figure 7**).

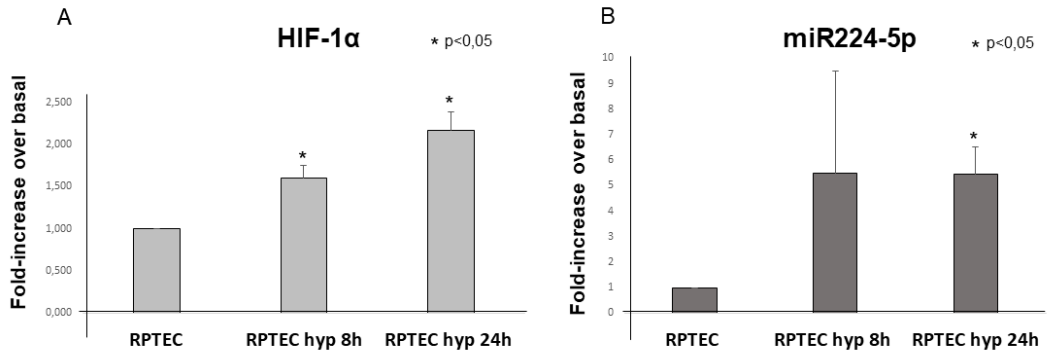

Figure 7: Expression of HIF-1α and miR-224-5p in hypoxic RPTEC lines
HIF-1α (A) and miR-224-5p (B) are significantly expressed by RPTEC exposed to 1% hypoxia compared to RPTEC at baseline (normoxia). The images are representative of 3 experiments. * vs RPTEC p<0,05.

Subsequently, and consistent with previous studies, increased PTX3 gene expression was observed in primary ccRCC lines when compared to RPTEC (12.75 ± 3.06 vs. 0.88 ± 0.16 UA; p <0, 05) (**Figure 8A**). However, we also noted increased expression of miR-224-5p in ccRCC cells compared to control cells (4.17 ± 0.83 vs. 0.32 ± 0.3 UA, p <0.05) (**Figure 8B**).

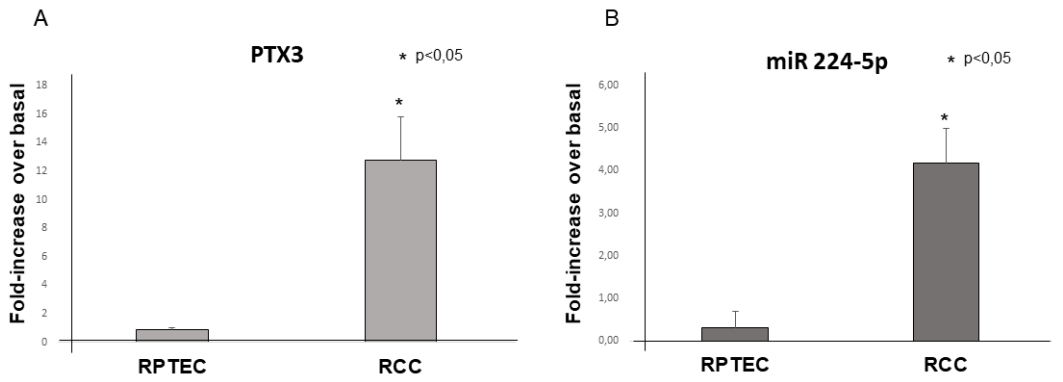

Figure 8: Expression of PTX3 and miR-224-5p in RCC and normal kidney cell lines
PTX3 is significantly expressed by several primary and immortalized renal tumor cell lines compared to primary and immortalized renal tubular cell lines (A).

Surprisingly, miR-224-5p was also highly expressed in RCC lines vs. RPTEC (B). The images are representative of 3 experiments. * vs RPTEC p<0,05.

To confirm these data, a gene expression analysis was performed on RNA extracted directly from tumors vs. patient-matched healthy kidney tissues in a cohort of 10 patients undergoing radical nephrectomy. Consistent with the *in vitro* analysis data, a coordinate increase in the gene expression of PTX3 and miR-224-5p was determined in ccRCC tumor tissues vs. normal, healthy tissues (**Figure 9A-B**).

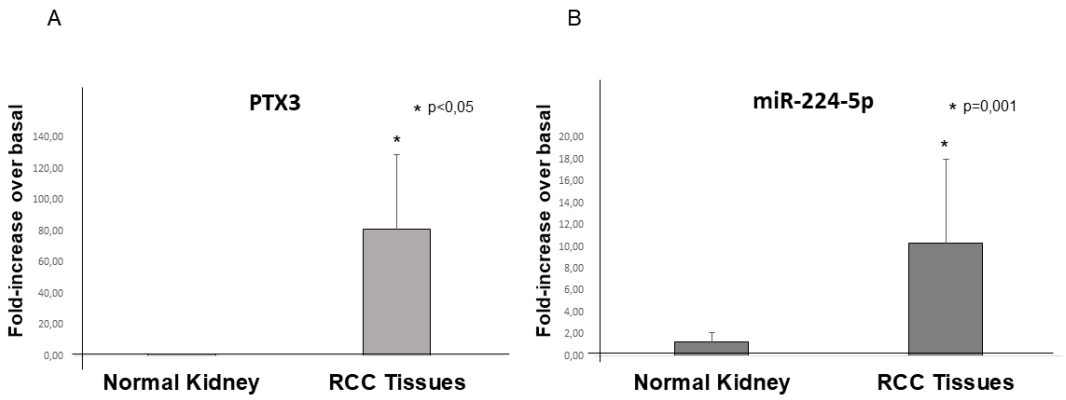

Figure 9: Expression of PTX3 and miR-224-5p in fresh ccRCC vs. patient-matched normal kidney tissue
Gene expression analysis confirms significant expression of PTX3 in ccRCC tissues compared to normal tissue (A). MiR-224-5p is also significantly elevated in ccRCC tissues compared to healthy kidney tissues (B). The presented data are representative of those obtained in 3 independent experiments. * vs normal kidney cells p<0,05.

4.1.3 PTX3 AND SASP GENE EXPRESSION IN TRANSFECTED RPTEC CELLS

To evaluate the correlation between PTX3 and miR-224-5p expression in renal cells, an *in vitro* functional analysis was conducted on RPTEC cells.

Preliminary experiments allowed us to establish optimal, non-toxic concentrations of the probe/lipid complex used for cell transfection.

The success of the transfection experiment was demonstrated by the observed increase in miR-224-5p gene expression in RPTEC cells transfected with the miR-224-5p mimic and by its reduction in RPTEC cells upon transfection with the putative inhibitory miR-224-5p (data not shown).

Consistent with our previous data obtained on tumor cells and tissues, functional analysis also revealed an increase in PTX3 gene expression in RPTEC cells transfected with the miR-224-5p mimic, however, this change was not statistically significant vs. the control.

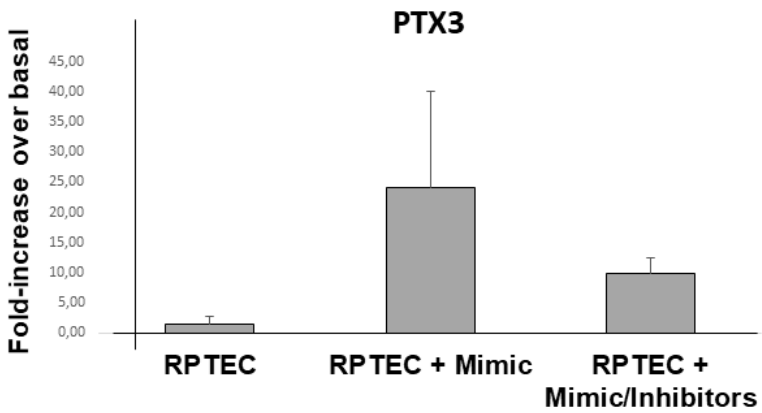

Figure 10: PTX3 expression is modulated in miR-224-5-p mimic transfected RPTEC cells

RPTEC cells transfected with the miR-224-5p mimic show an increase in the PTX3 gene expression signal which is reduced in RPTEC cells cotransfected with the mimic and a specific miR-224-5p inhibitor.

Analogous results were obtained in confocal microscopy analyses when comparing the various transfected cells, with expression of PTX3 significantly increased in RPTEC cells transfected with the miR-224-5p mimic when compared to basal RPTEC cells (**Figure 11**).

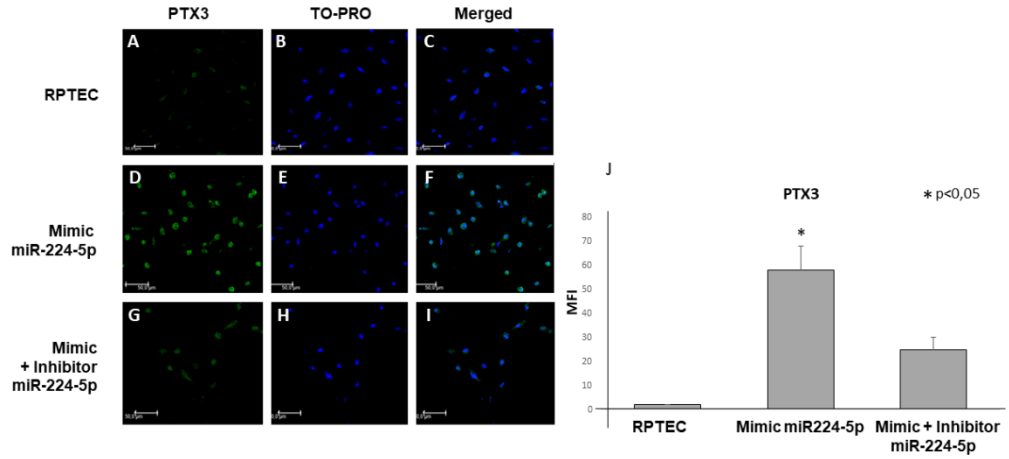

Figure 11: PTX3 expression in RPTEC cells transfected with the miR-224-5p mimic
Confocal microscopy images show significant PTX3 (green) expression in RPTEC cells transfected with miR-224-5p mimic compared to the baseline condition (A-B). A reduction of the expression signal is observed in RPTEC cells cotransfected with the miR-224-5p mimic + its specific inhibitor. The images are representative of those obtained in 3 independent experiments. Cell nuclei are staining with TO-PRO-3 (blue). (Bar = 50 microns; Objective 40x oil immersion - Magnification 400x). Fluorescence quantification analysis (* vs RPTEC $p<0.05$) is reported (J).

The same transfection assay was conducted to evaluate changes in target cell expression of SASP-related markers (i.e., IL-6, p21, p16). The resultant analysis showed that upregulation of miR-224-5p leads to a non significant increase in the inflammatory signals linked to SASP in mimic-transfected vs. control RPTEC cells (**Figures 12-14**).

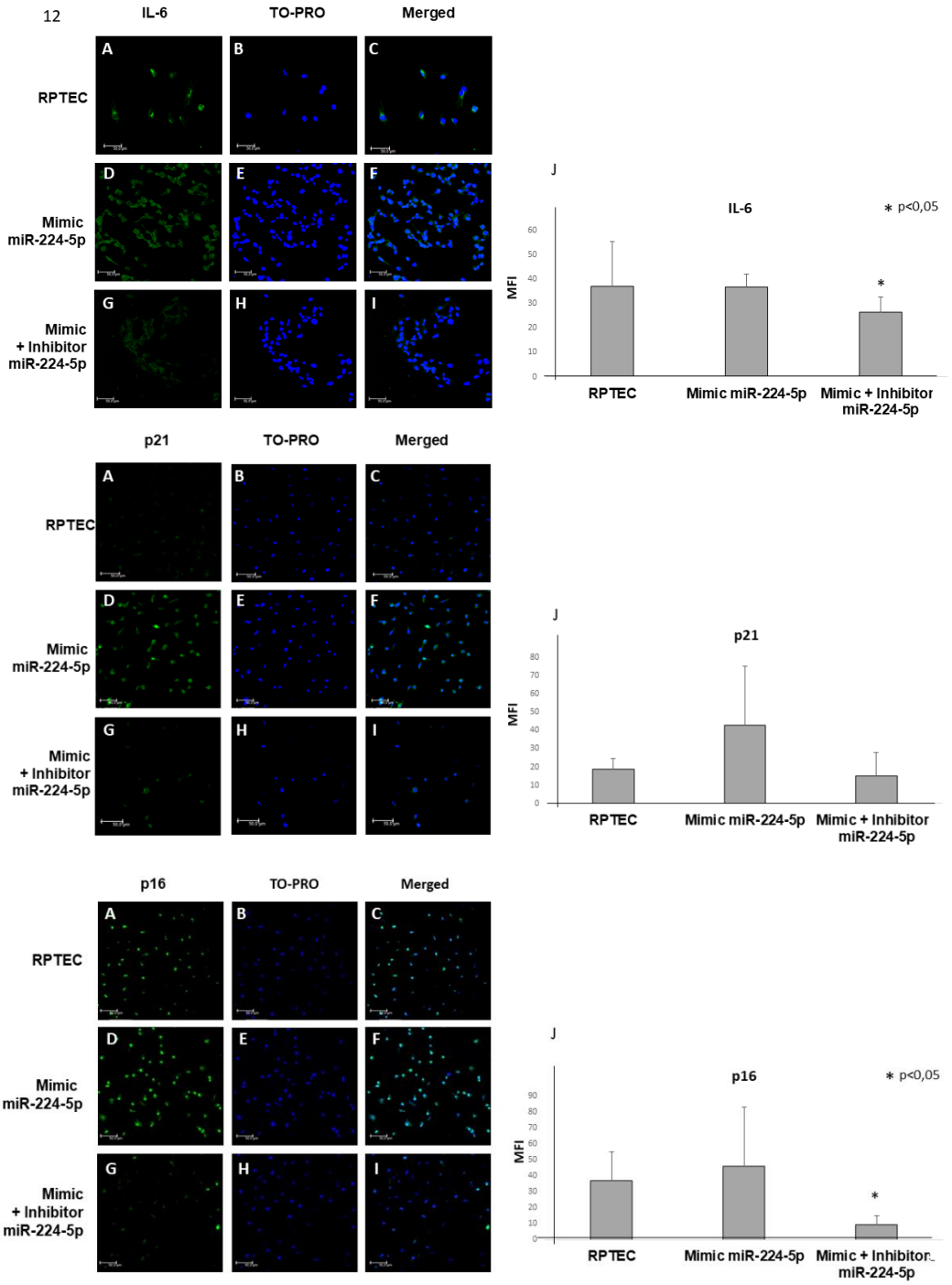

Figure 12: SASP-associated protein expression in RPTEC cells transfected with the miR-224-5p mimic

IL-6, p21 and p16 (green) protein expression was investigated by IFM in RPTEC cells transfected with miR-224-5p mimic compared to control, untransfected cells (Upper, medium, lower panel D-F). A reduction in SASP-associated protein expression was observed in RPTEC cells transfected with the miR-224-5p mimic + its specific inhibitor (Upper, medium, lower panel G-I). Cell nuclei are staining with TO-PRO-3 (blue). Fluorescence quantification analysis ($p<0.05$) is reported in upper, medium, lower panels J.

4.2 PTX3 AND SASP EXPRESSION IN HYPOXIC CELL LINES

To better mimic the RCC TME, RPTEC and immortalized RCC cells were exposed to hypoxia conditions *in vitro*. Although absent at basal conditions, after culture under conditions of 1% hypoxia, expression of PTX3 and IL-6 was significantly and progressively increased in RPTEC and RCC cell lines in a time-dependent manner. Interestingly, expression of SASP-associated p21 and p16 were upregulated in hypoxic RPTEC while in RCC cell lines, p21 was similarly expressed to baseline condition of RPTEC and p16 expression was undetectable (**Figure 13**).

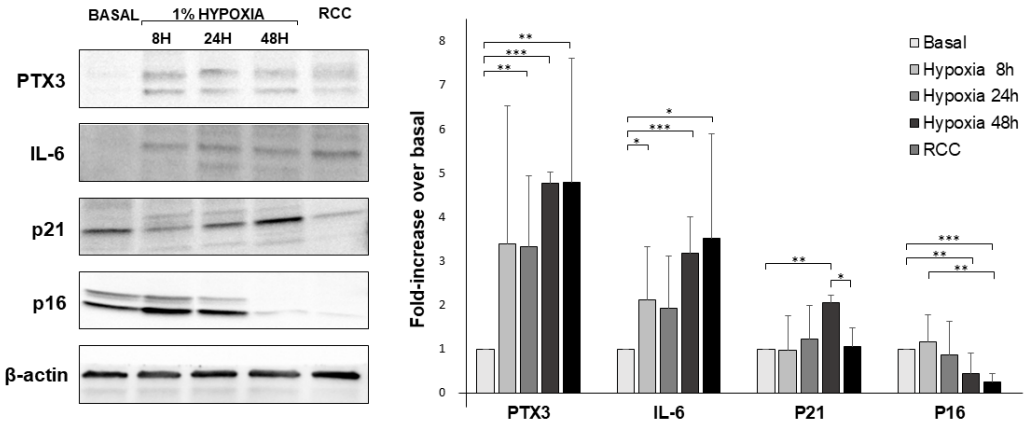

Figure 13: PTX3 and SASP-related proteins expression in renal cell lines

In A, expression of PTX3 and IL-6 were significantly and progressively increased in hypoxic RPTEC and remained significantly increased also in RCC cells compared to RPTEC at baseline (Western Blot). Cell-cycle inhibitors increased in hypoxic RPTEC compared to RPTEC at baseline. In RCC cells, p21 expression was similar to baseline condition of RPTEC and p16 was undetectable. In B, protein bands were quantified and reported in a.u. relative to control, as mean ± SD. The presented data are representative of those obtained in three independent experiments performed. (*p≤0,05; **p≤0,01; ***p≤0,001).

4.3 ANALYSIS OF INFLAMMAGING IN PERITUMORAL AND TUMOR REGIONS IN RCC TISSUES

4.3.1 PTX3 EXPRESSION IN PERITUMORAL AND TUMOR REGIONS OF RCC TISSUES

The analysis of tissue expression by confocal microscopy revealed a progressive and significant increase in PTX3 expression both in peritumoral areas and in the tumor core of patients with ccRCC compared to patient-matched normal kidney tissues ($p<0.001$) (**Figure 14**).

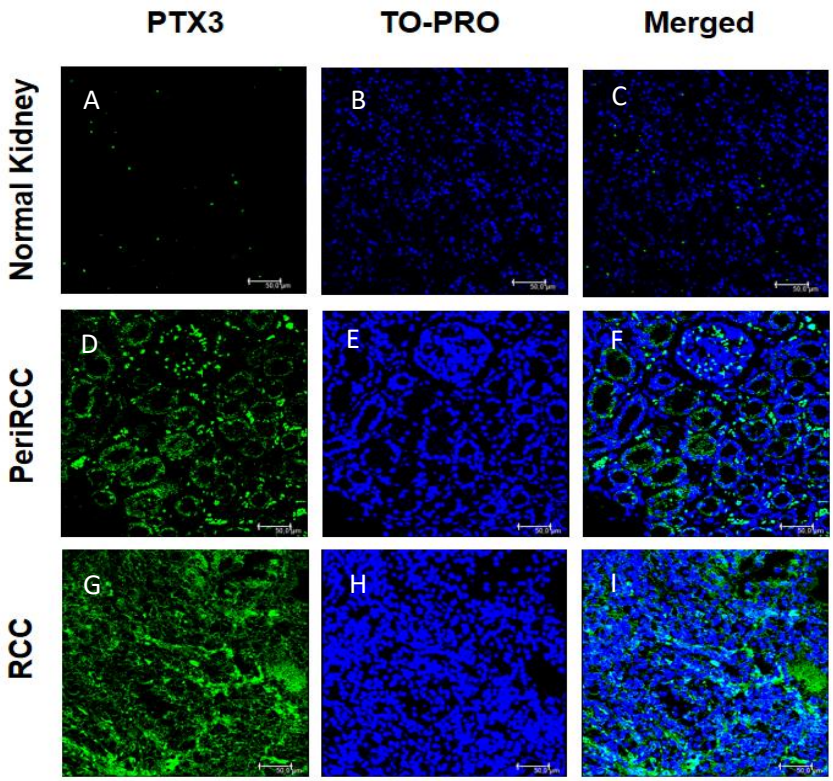

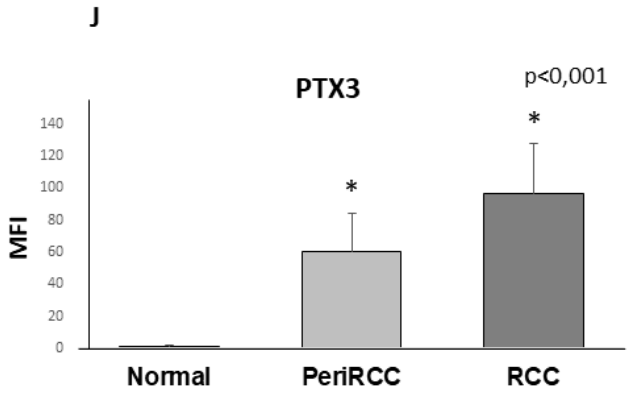

Figure 14: PTX3 expression in peritumoral and RCC tumor tissue.
Based on IFM analyses, expression of PTX3 (green) is elevated over normal kidney tissue (A-C) in both peritumoral (D-F) and intratumoral (G-I) regions of resected RCC patient tissues. The images presented are representative of data obtained in 3 independent experiments involving study of 10 unrelated patients. The nuclei are stained with TO-PRO-3 (blue). (Bar = 50 micron - 40x oil immersion objective - 400x magnification) Fluorescence quantification analysis (* vs normal kidney $p<0.001$) is reported (J).

4.3.2 SENESCENCE SIGNATURES IN "HEALTHY" RENAL TISSUES

SA-β-Gal Staining was performed to evaluate the senescent nature of healthy, normal kidney tissue. A feature of senescent cells is the increased activity of this enzyme. Surprisingly, the enzymatic assay allowed us to detect significant activity of SA-β-Gal at pH 6 in healthy renal tissue vs. RCC tissue which failed to express this senescence-associated biomarker (**Figure 15**).

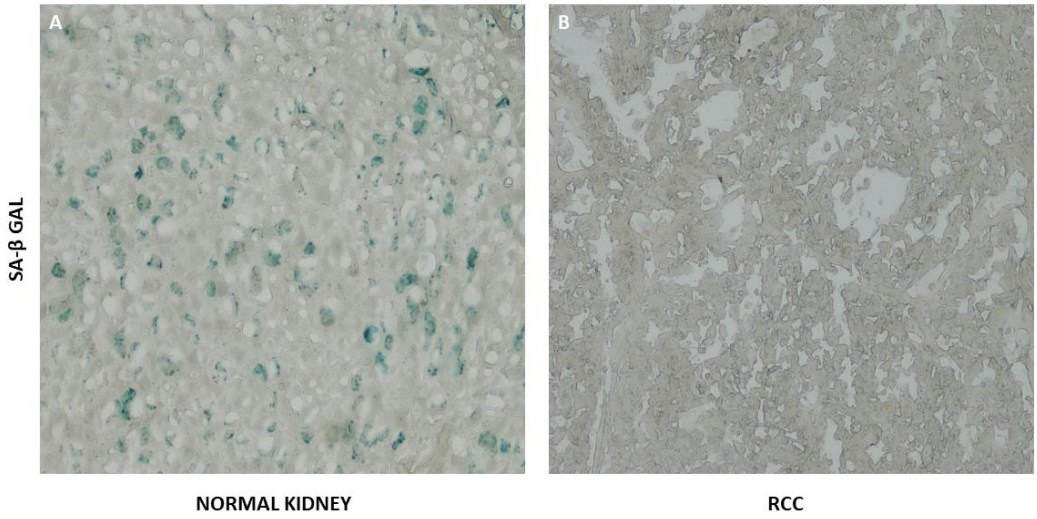

Figure 15: SA-β-gal staining in normal renal tissue vs. RCC
(A) Histopathologically normal and healthy renal tissues stained positive for SA-β-Gal enzymatic activity (blue). (B) RCC tissues failed to exhibit SA-β-Gal enzymatic activity, suggesting that they lack characteristics of senescence. Representative images are acquired by phase contrast microscopy (Magnification 10x).

4.3.3 TISSUE EXPRESSION ANALYSIS OF INFLAMMAGING MARKERS

We next conducted an analysis to correlate PTX3 expression to SASP marker expression in RCC vs. normal kidney specimens. We observed that PTX3 and IL-6 were strongly expressed in peritumoral areas and tumor regions of RCC compared to normal tissue ($p<0.001$) (**Figure 16**). PTX3 expression colocalized with expression of the p21 and p16 markers of SASP, mainly in kidney tubular structures. Interestingly, while PTX3 expression appeared greater in peritumoral vs. core tumor tissues, p16 and p21 expression was more evident in peritumoral tissue ($p<0.001$) but decreased in tumor tissue ($p=0.01$) when compared to normal kidney tissue (**Figure 16**)

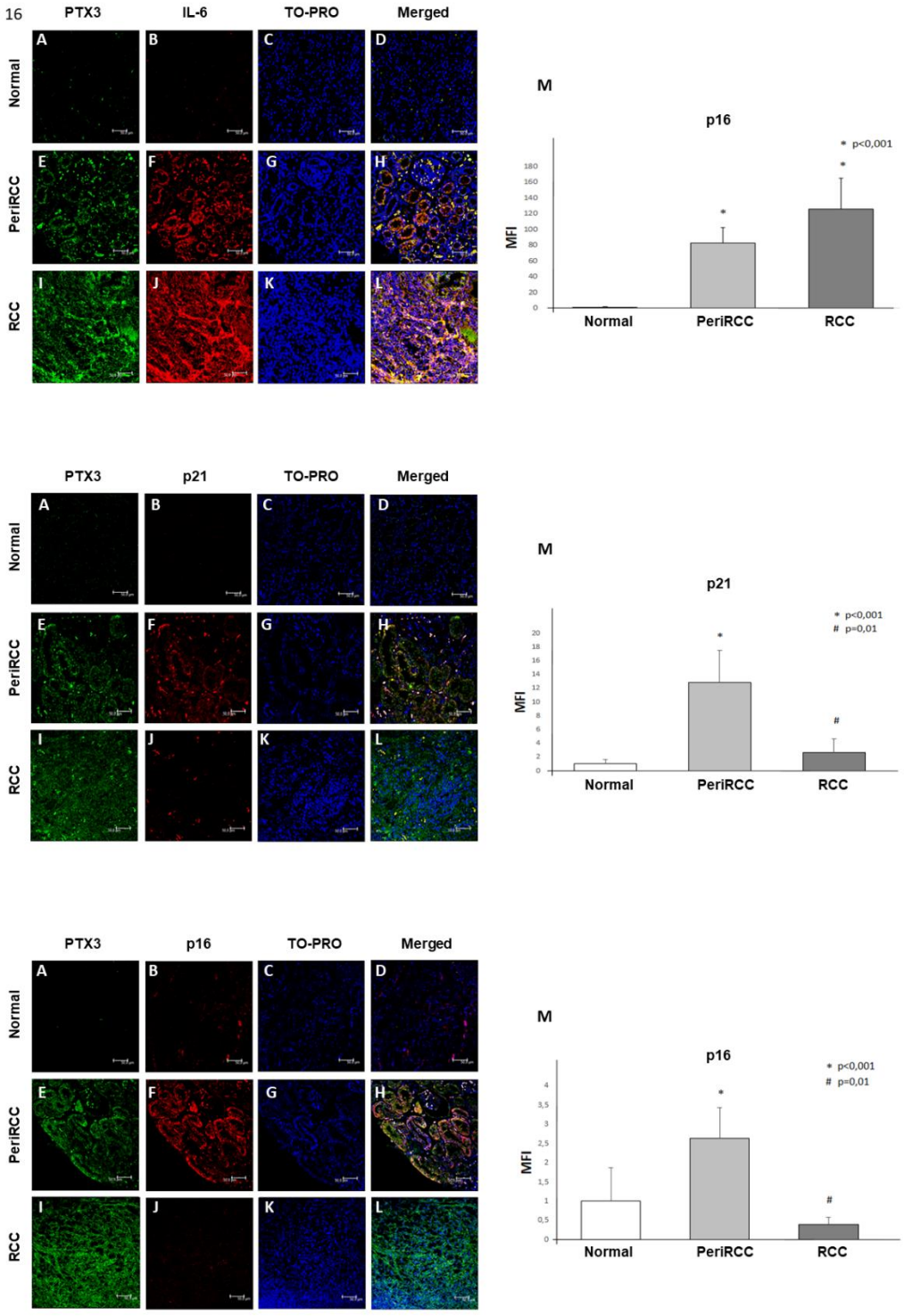

Figure 16: Expression of PTX3 and SASP related proteins in peritumoral and tumor tissue regions of RCC versus normal kidney tissue.

Expression of PTX3 (green) and IL-6 (red) determined by IFM shows a significant elevation in RCC peritumoral (upper panel, E-H) and tumor (upper panel, I-L) tissue regions when compared to normal kidney tissue. PTX3 (green) expression

colocalizes with expression of the SASP-associated cell cycle inhibitors, p21 and p16 (red). Expression of p21 and p16 is increased in peritumoral tissues (medium and lower panel, E-H), but reduced in tumor tissue (medium and lower panel I-L) when compared to normal tissue. Nuclei are stained with TO-PRO3 (blue). Fluorescence quantification analysis ($p<0.001$ peritumoral vs normal; $p=0.01$ tumor vs. normal) (upper, medium and lower panel, M) is reported. Data are representative of 10 RCC specimens isolated from independent patients.

Since p16 was quantitatively expressed to a higher degree compared to p21 in peritumoral tissues, a further analysis was performed to evaluate the phenotype of p16 positive cells. The results obtained showed that senescent cells in peritumoral tissue coordinately express high levels of both p16 and IL-6 when compared to normal kidney tissue. In tumor tissues, IL-6 expression remained elevated, in deference to p16 expression levels (**Figure 17**). These data suggest that cancer tissues may lose control of the cell cycle in favor of the (pro-tumor) inflammatory process.

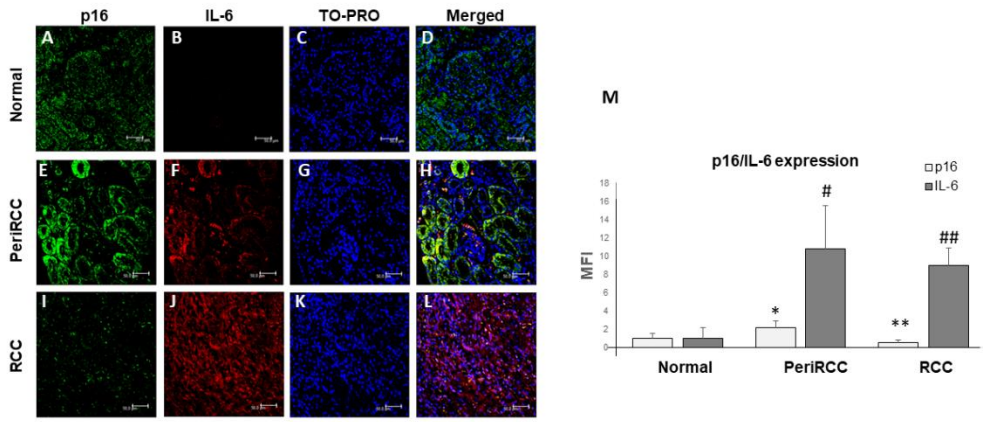

Figure 17: IFM evaluation of the SASP phenotype in peritumor and tumor tissue of RCC.
P16 (green) colocalizes with the inflammatory marker IL-6 (red). The expression of p16 and IL-6 is increased in peritumoral RCC tissue compared to normal kidney tissue (E-H). In RCC tumor tissue only the expression of IL-6 is elevated (J-L), while the expression of p16 is decreased vs. control tissue (I-L). Nuclei are stained with TO-PRO-3 (blue). Fluorescence quantification analysis of both p16 and IL-6 expression on normal kidney tissue, peritumoral renal tissue and RCC (p16 * vs basal $p<0.001$, ** vs basal $p=0.01$, + vs ** $p<0.001$; IL-6 # vs basal $p<0.001$, ## vs basal $p<0.001$, # vs ## p=ns).

4.3.4 SASP MODULATION ACCORDING TO FUHRMAN GRADING IN RCC PERITUMORAL AND TUMOR TISSUES

An analysis of the expression of inflammaging markers was conducted as a function of Fuhrman grading (WHO/ISUP grading system, Eur Urol 2016). Expression of PTX3 was increased in the peritumoral and tumor tissues of patients with high-grade RCC (G3-G4) compared to the peritumoral and tumor tissues of patients with low-grade RCC (G1-G2) (**Figure 18**).

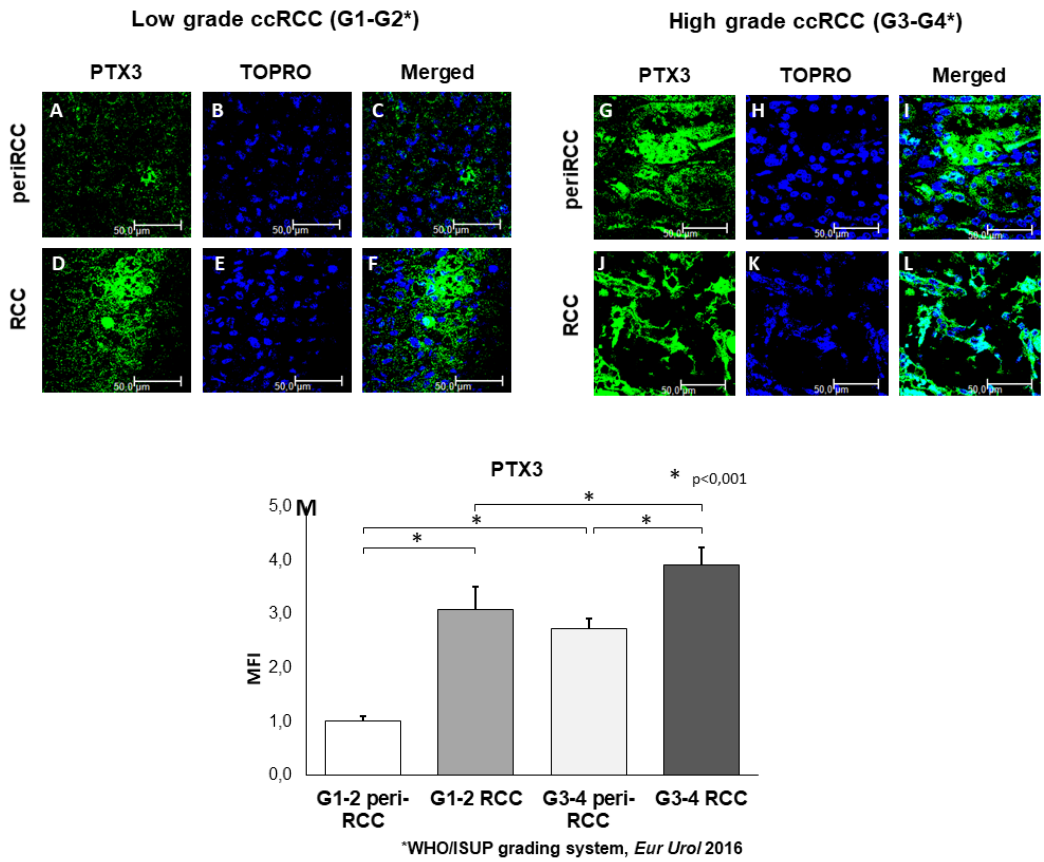

Figure 18: PTX3 expression in peritumoral and tumor regions of RCC increases as a function of Fuhrman grade.
IFM analysis of RCC specimens was performed revealing that expression of PTX3 (green) is increased in the peritumoral (G-I) and tumor core (J-L) regions of high-grade tumors vs. the peritumoral (A-C) and tumor core (D-F) regions of low-grade tumors. Nuclei are stained with TO-PRO-3 (blue). In (M), fluorescence quantification analysis of the indicated IFM cohorts is reported (*p<0.001).

Like PTX3, IL-6 is also more highly expressed in the peritumoral and tumor core regions of high-grade vs. low-grade RCC (**Figure 19**).

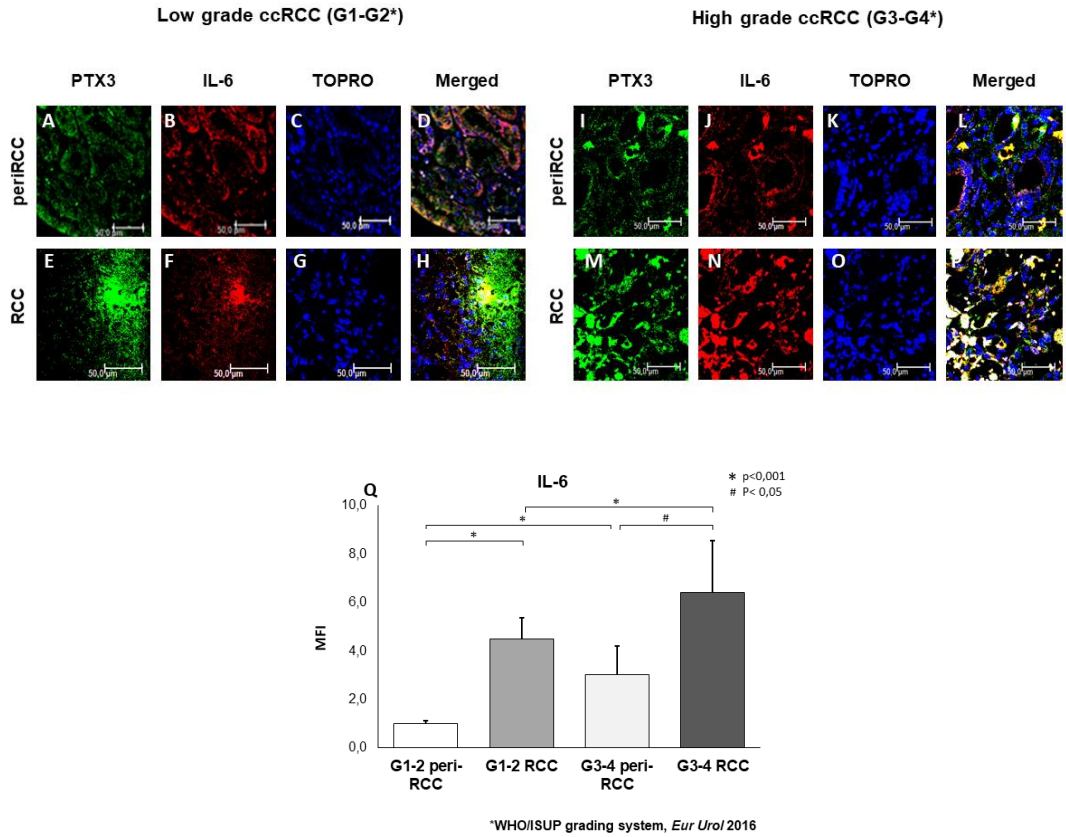

Figure 19: Differential IL-6 expression in the peritumoral and tumor core regions of RCC relates to Fuhrman grade.
The expression of PTX3 (green) and IL-6 (red) is elevated in the peritumoral (I-L) and tumor core (M-P) regions of high-grade RCC when compared to the peritumoral (A-D) and tumor core (E-H) regions of low-grade RCC. Nuclei are stained with TO-PRO-3 (blue). Fluorescence quantification analysis (*p<0.001 #p<0,05) (Q) is reported.

By extending the analysis to expression of cell cycle inhibitors, we observed that p21 and p16 were similarly expressed in high and low grade peritumoral

tissues. In tumor tissues however, expression of these cell cycle inhibitors was reduced in high-grade tumors vs. low-grade tumors (**Figures 20**).

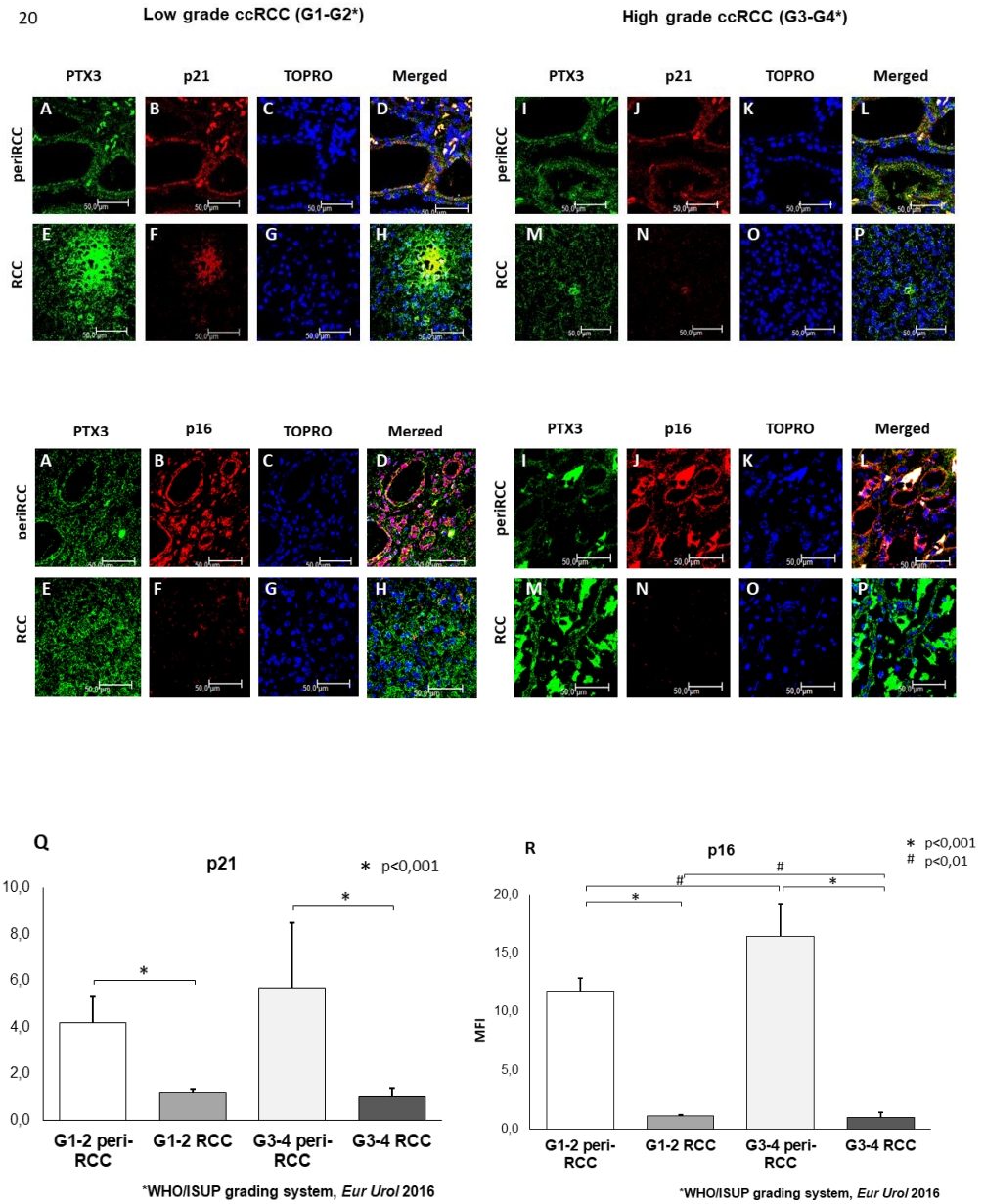

Figure 20: Expression of p21/p16 in peritumoral and tumor core regions of RCC as a function of Fuhrman grade.

Expression of PTX3 (green) and p21/p16 (red) is increased in the peritumoral regions of high-grade tumors (Upper and medium panel, I-L) compared to the corresponding peritumoral regions of low-grade tumors (Upper and medium panel, A-D). In marked contrast, expression of p21/p16 decreases significantly in high-grade tumor core tissues ($p<0.05$) (Upper and medium panel, M-P)

compared to low-grade tumor core tissues (Upper and medium panel, I-H). Nuclei are stained with TO-PRO-3 (blue). Fluorescence quantification analysis (*p<0.001 #p<0,01) (Q-R) is reported.

Further evaluation of the phenotype of p16 positive cells suggests that peritumoral and tumor core regions of high-grade RCC are enriched in a SASP phenotype when compared with corresponding regions in low-grade RCC (**Figure 21**).

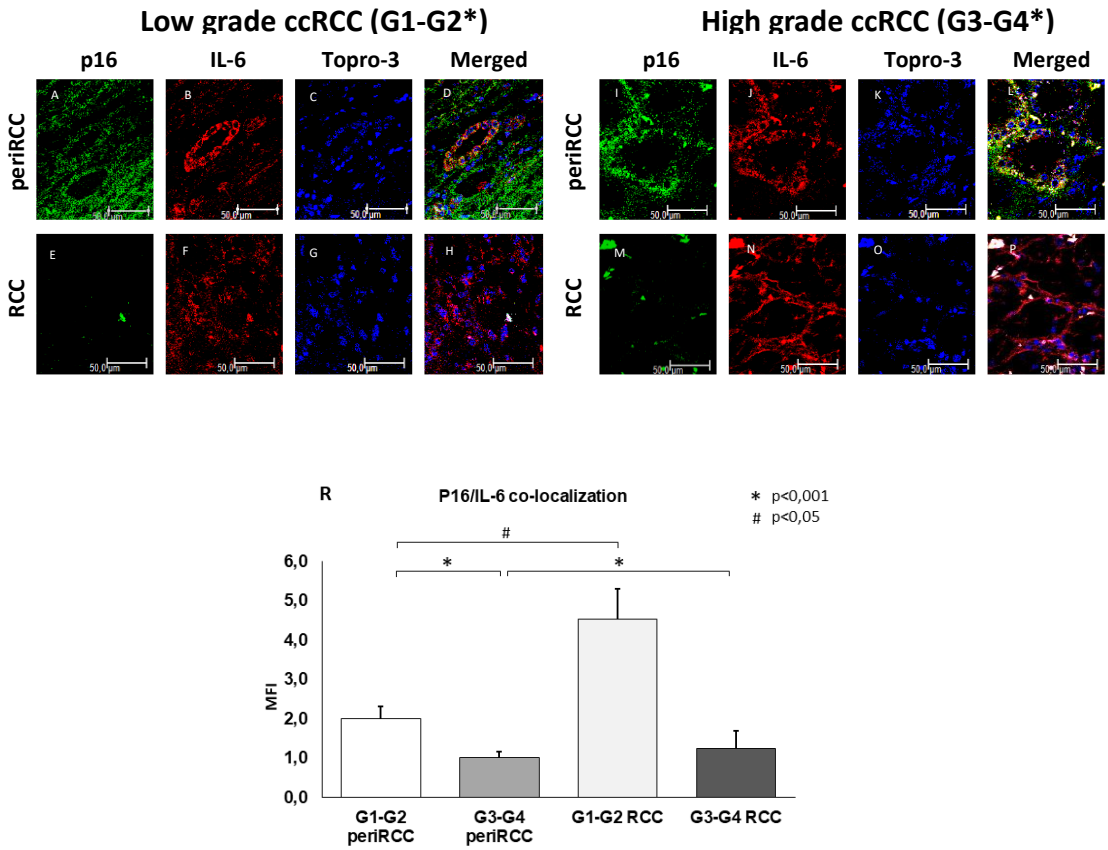

Figure 21: Evaluation of the SASP phenotype in peritumoral and tumor core regions of RCC according to Fuhrman grading

P16 (green) expression colocalizes with expression of the inflammatory cytokine IL-6 (red) in IFM analyses of RCC specimens. Expression of p16 and IL-6 is increased in the peritumoral regions of high-grade RCC (I-L) when compared to corresponding regions in low-grade RCC (A-D). In tumor core tissues, only IL-6 expression remains elevated and is more evident in high-grade tumors (N-P) than in low-grade tumors (F-H). The nuclei are stained with TO-PRO-3 (blue). (Q) Fluoresence quantification of p16/IL-6 colocalization (yellow signal) (*p<0,001 #p<0,05)

5. DISCUSSION

The present thesis study represents the first investigation of inflammaging mechanisms in the setting of RCC.

Previous work from our group highlighted the finding for increased expression of PTX3 in sera and tissues of ccRCC patients and the utility of PTX3 as a biomarker of inflammation that impacts the TME and ccRCC progression.

Our observation for progressively increased expression of inflammatory markers in RPTEC and RCC and decreased expression of cell-cycle inhibitors in RCC cells compared to normal kidney tubular cell lines by immunoblotting analysis triggered further investigation of how inflammaging mechanisms were impacted by conditions of hypoxia in RCC.

These results reinforce the idea that senescence activation is also correlated to the activation of a pro-tumor systems biology characterized by hypoxia and angiogenesis that facilitates disease progression.

Our qRT-PCR analyses showed an increase in PTX3 gene expression in RCC compared to control normal kidney lines and tissues. Through *in silico* analyses, a study of the literature and gene expression analyses, we identified miR-224-5p as a potential regulator of PTX3 expression in RCC.

Several studies have shown that miR-224-5p plays an important role in the pathogenesis of various cancers. MiR-224-5p is upregulated in cancers of the digestive tract where it coordinately serves as a diagnostic and

prognostic biomarker [140]. In esophageal cancer and non-small cell lung cancer, miR-224-5p promotes tumor proliferation, migration and invasiveness, acting as an oncogenic miRNA [141, 142]. In meningioma, this miR supports tumor proliferation and survival via suppression of apoptosis [143].

In this thesis project, we observed increased expression of miR-224-5p in ccRCC tumor cells and tissues, consistent with literature findings for increased miR-224-5p expression in extracellular urinary vesicles isolated from patients with RCC [144] and for an association between expression of this miRNA with ccRCC proliferation, migration and invasiveness [144, 145].

MiR-224-5p has been reported to be hypoxia responsive in the setting of melanoma and gastric carcinoma [146, 147]. In particular, the study by Chuan and colleagues demonstrated the existence of an HRE region upstream of the precursor transcript of miR-224-5p. Given the high percentage of mutations affecting the VHL gene leading to stabilization of HIF-1α in RCC, it is plausible to hypothesize that the induction of this miRNA is conditioned by local hypoxia in the TME. By definition, miRNAs are small non-coding endogenous RNAs that regulate gene expression both at the transcriptional and post-transcriptional level, by binding to the target mRNA and consequently promoting their translation, repression or degradation.

Thus, in theory, increased expression of a given miRNA in cells corresponds to reduced expression of a range of target mRNAs/proteins within those

same cells. In fact, several studies have investigated the role of miR-224-5p in directly or indirectly modulating expression of PTX3. In the study by Li and colleagues, it was observed that, in cumulus oophore cells, increased expression of miR-224 was associated with a reduction in PTX3 expression, with corollary effects observed on fertility and oocyte development [148]. In a study on cervical cancer, increased miR-224 expression was observed in cancer patients with a corresponding decrease in PTX3 levels, with both trends linked to poor clinical prognosis [150]. Furthermore, down-regulation of miR-224 expression and increased PTX3 expression has been reported in the setting of prostate cancer in association with poor clinical outcomes [150].

In contrast to these papers, the current study reports a coordinate increase in both miR-224 and PTX3 in RCC cells and tissues.

In this context, it is important to note that a study relating to inflammation of the inner ear reported down-regulated expression of PTX3 by miRNA 224 in normal baseline tissue, while expression of both factors was increased after treatment with an inflammatory stimulus. The authors supported the theory that induction of PTX3 expression as a consequence of local inflammation leads to a (compensatory) increase in miR-224 expression to restore basal levels of PTX3 via a feedback regulatory mechanism [151]. Recent studies have also suggest that miRNAs can interact with the target mRNA promoter regions leading to activation in gene expression [152]. Although miRNAs are theoretically present only in the cytoplasm in their mature form, it has been further hypothesized that some miRNAs are also

present in the nucleus of cells where they may function as enhancers of gene expression. [153].

This mechanism, called RNA activation (RNAa), is a transcriptional activation process in which the direct interaction of miRNA with a gene promoter triggers the recruitment of transcription factors and RNA-polymerase-II leading to activation of gene transcription. Transcriptional activation can affect cells in a contextual manner based on cellular state of quiescence, nutrient scarcity or by binding to the 5 'UTR region of target gene products [154].

We readily acknowledge limitations in the current studies; i.e., the small number of patients analyzed. This makes the current pilot studies primarily hypothesis-generating, namely, that increased, coordinate expression of miR-224-5p and PTX3 plays an important role in RCC pathobiology. Furthermore, we posit that miR-224-5p upregulation positively impacts the process of inflammaging that underlies RCC-associated disease progression.

In these thesis studies, we also extended our analyses to include a characterization of peritumoral tissue in the RCC TME, noting for the first time a progressive increase in PTX3 expression from normal to peritumoral tissue to tumor tissue. Peritumoral tissue is considered a transition tissue, marginal to the tumor, in which different mechanisms converge to promote the arrest of cancer evolution and/or to foster its progression. Peritumoral tissue, surrounding the tumor, provides a proper environment (i.e., soil) for tumor cell growth at the leading edge of the disease mass. This peritumoral

microenvironment (PME) represents an emerging site for studies designed to better understand tumor biology and to design targeted interventions for improved patient benefit.

The occurrence, recurrence and metastasis of tumor is strongly dependent on PME and TME composition and their functional characteristics [155]. The complexity of the TME is reflected not only in the genetic and phenotypic heterogeneity of cancer cells, but also in the profile of infiltrated/resident immune cells and inflammatory mediators located within the stroma that defines the so-called inflammatory TME. These are closely involved in all stages of cancer development, including initiation, promotion and progression. Indeed, an inflammatory PME appears directly related to tumorigenic potential [156]. Hence the presence of immune cells/inflammation in the TME is increasingly recognised as a double-edged sword that on the one hand promotes neoplastic proliferation and, on the other hand, may be harnessed to promote therapeutic clinical benefit by restricting tumor growth and metastasis mediated in part via improved immune surveillance [157, 158].

In addition to inflammation, senescence also showed a variable, context-dependent role in ccRCC pathogenesis. Senescence is generally considered a process of cell cycle arrest with a suppressive function that limits the proliferation of cancer and/or damaged cells. Nonetheless, it can also promote the development of cancer by enriching the TME with a particular secretory phenotype called SASP, mainly characterized by increased expression of cell cycle inhibitors and proinflammatory cytokines. Indeed, in contrast to apoptotic and quiescent cells, senescent cells exhibit high

metabolic activity which may stem from SASP. It is argued that the occurrence of SASP may explain why a relatively small number of senescent cells can have powerful local and systemic effects promoting aging phenotypes and disease-associated pathologies [159].

In our study, we observed for the first time an intriguing association between PTX3 and SASP marker expression in ccRCC, both in peritumoral and tumor core regions of RCC. Increased expression of PTX3 was associated with an increase in expression of IL-6, confirming the highly inflammatory nature of the ccRCC TME. Regarding the expression of cell cycle inhibitors, we observed an increase in expression of p21 and p16 primarily in peritumoral areas, with reduced expression of these protein in tumor core areas. We subsequently observed that in the classification according to the Fuhrman grading, high-grade and therefore more poorly-differentiated tumors exhibited higher levels of inflammatory cytokines and a lower level of cell-cycle inhibitor expression vs. more differentiated tumors. This was true in both the peritumoral and tumor core regions of RCC lesions. P21 and p16 are expressed by proximal tubular cells where they appear to maintain a state of physiological senescence to prevent DNA damage [160]. An alteration in the expression of p21 and p16 correlates with the progression of cancer [161]. Almost 50% of human cancers show p16 inactivation [161, 162, 163, 164]. Within ccRCC, expression of p21 and p16 has prognostic significance. When expressed at low levels, p21 correlates with metastatic forms of ccRCC, while higher levels of p21 expression correlate with localized forms of ccRCC [165]. Even reduced expression of p16 seems to be associated with more aggressive forms of cancer, with a

single showing in a tissue analysis of 397 nephrectomy specimens that low expression of p16 correlates with poorer patient survival [166].

In addition, our confocal microscopy analyses revealed a higher expression of p16 vs. p21 in peritumoral areas. However, based on the available scientific evidence, p21 is required for the induction of senescence, while p16 maintains cell cycle arrest over extended periods of time [95]. In light of these considerations, we evaluated whether the SASP phenotype is acquired in p16 positive cells. Our studies showed a correlation between p16 and IL-6 expression and in particular, an increase of both signals in peritumoral regions of RCC. Interestingly, tumor core regions of RCC were selectively characterized by a selective increase in IL-6 expression. These data support the hypothesis that a loss of control in cell cycle arrest within the tumor core favors an inflammatory TME.

It is now well documented that the increased expression of p16 and SASP are characteristics of oncogene-induced senescence (OIS). While increased p16 expression promotes characteristic cell cycle arrest [167, 168], SASP appears to be a consequence of the DNA damage response induced by OIS and is not necessary for proliferative arrest [169, 170].

Several studies have reported that decreased p16 expression leads to a reduction in IL-6 secretion by senescent cells [171, 172, 173]. This finding is consistent with the current thesis data, where we observed that p16/IL-6 expression according to Fuhrman grading is reduced principally in peritumoral tissue regions.

Within the tumor core tissue, we observed a decrease of p16 expression which was not paralleled by a reduction in IL-6 expression. Hence these thesis studies report for the first time that peritumoral tissue appears to develop a senescent state. This occurs arguably in an attempt to counteract malignant transformation by promoting cell cycle arrest and coordinate acquisition of an SASP phenotype (based on increased secretion of IL-6 and elevated expression of PTX3), thereby modulating the proliferative status of tumor cells at the leading edge of cancer lesions.

IL-6 has been frequently studied in RCC, with elevated IL-6 serum levels reported in 25% of patients with RCC and in more than 50% of patients with metastatic renal cell carcinoma [174, 175]. High levels of IL-6 in RCC patient serum has been associated with poor survival and resistance to interventional drug treatment [176].

Recent studies have focused on the role of PTX3 in inflammaging [177, 178]. PTX3 is an inflammatory molecule that appears to play a critical role in tumor progression. Although a link with senescence remains to be fully explored, in line with our data, a recent study in the setting of gliomas found that patients with high-grade cancers displayed increased PTX3 expression levels compared to patients with low-grade disease. Surprisingly, the authors noted that knockdown of PTX3 gene expression inhibits tumor cell proliferation by increasing levels of p21 protein expression and by downregulating expression of metalloproteinases, leading to cell cycle arrest [179].

In addition to tumor cells, the TME of ccRCC contains several lymphoid and myeloid cell subpopulations as well as myofibroblasts and endothelial cells. Although fundamentally similar to other tumors, RCC typically contains a strong leukocyte infiltrate and abundant vascularization, supported by a high local expression of VEGF, one of the downstream targets of the HIF-1 and HIF-2 transcription factors [180]. As previously reported by others [19], in 40% of ccRCC cases a deletion of the HIF-1 locus occurs allowing the classification of tumors into two phenotypes: H1H2 vs. H2 [180]. In our study, we observed an association between increase expression of PTX3 and HIF-1/HIF-2-dependent factors in peritumoral and tumor core regions of RCC.

A limitation of these latter studies in this thesis reflects the fact that within the context of tissue analyses, positivity for inflammaging markers was not cell type-specific. Hence, further investigation is required to provide a better understanding of whether the observed senescence in the TME is related more to cancer cells or stromal cells in influencing the evolving PME/TME in RCC in impactingtumor control vs. disease progression.

6.CONCLUSIONS

This study paves the way to an improved understanding of inflammaging as a mechanism impacting ccRCC disease progression.

We demonstrated for the first time that increased expression of PTX3 in ccRCC cells and tissues corresponds to increased expression of miR-224-5p. Considering the pleiotropic nature of miRNAs, especially in the oncology field, our transfection analyses are informative in demonstrating an intriguing and likely impactful positive correlation between miR-224-5p and target PTX3 expression. Although prospective molecular studies are needed, it is plausible to hypothesize that these interactive biomarkers represent important components of an RCC disease-associated operating module.

Furthermore, this study highlights for the first time reports operational differences in the senescence status of peritumoral vs. tumor core RCC tissues. Indeed, peritumoral tissue appears to develop a senescent state arguably in the attempt to counteract malignant transformation by promoting cell cycle arrest and coordinate acquisition of an SASP phenotype characterized by increased secretion of IL-6 and elevated expression of PTX3 that influence cellular proliferative in the TME.

Coordinate targeting of complementary pathways in the PME and TME may provide unique and effective future opportunities for RCC diagnosis, prevention and treatment.

7.REFERENCES

1. Mydlo J. Growth factors and renal cancer: Characterization and therapeutic implications. World J. Urol. 1995; 13: 356–363.
2. Decastro GJ, McKiernan et al. clinical staging, and presentation of renal cell carcinoma. Urol Clin North Am. 2008; 35(4): 581-92;
3. Cohen HT, McGovern FJ. Renal-Cell Carcinoma. N. Engl. J. Med. 2005; 353: 2477–2490.
4. Schena FP, Selvaggi L, Gesualdo M, et al. Malattie del Rene e Delle Vie Urinary. 4th ed. McGraw-Hill; New York, NY, USA: 2008.
5. Gibbons RP, Monte JE et al. Manifestations of renal cell carcinoma. Urology. 1976; 8 (3):201-6.
6. Chow WH, Dong LM et al. Epidemiology and risk factors for kidney cancer. Nat Rev Urol 2010; (7):245-57.
7. Hutson TE. Targeted therapies for the treatment of metastatic renal cell carcinoma: clinical evidence. Oncologist. 2011;16:14-22.
8. Rini B, Campbell SC, Escudier B. Renal cell carcinoma. Lancet. 2009; 373:1119–1132.
9. Vavallo A, Simone S, Lucarelli G, et al. Pre-existing Type 2 Diabetes Mellitus Is an Independent Risk Factor for Mortality and Progression in Patients with Renal Cell Carcinoma. Medicine. 2014; 93:e183.
10. Kierstead LS, Ranieri E, Olson W, et al. gp100/pmel17 and tyrosinase encode multiple epitopes recognized by Th1-type CD4+T cells. Br. J. Cancer. 2001; 85:1738–1745.
11. Chen YB, Xu J, Skanderup AJ, et al. Molecular analysis of aggressive renal cell carcinoma with unclassified histology reveals distinct subsets. Nat. Commun. 2016; 7:1–10.
12. Cairns P. Renal. cell carcinoma. Cancer Biomark. 2010; 9(1-6):461-473.
13. Loboda A, Jozkowicz A, Dulak J. HIF-1 and HIF-2 transcription factors—similar but not identical. Mol Cells. 2010; 29(5):435-42.

14. Pavlovich CP, Schmidt LS, Philips JL. The genetic basis of renal cell carcinoma. Urol Clin North Am. 2003 Aug;30(3):437-54.
15. Maher ER, Yates JR, Harries R. Clinical features and natural history of von Hippel-Lindau disease. Q J Med. 1990; 77(283):1151-63,
16. Koshiji M, Kageyama Y, Pete EA, et al. HIF-1alpha induces cell cycle arrest by functionally counteracting Myc. EMBO J. 2004; 23(9):1949-56
17. Loboda A, Jozkowicz A, Dulak J. HIF-1 versus HIF-2--is one more important than the other? Vascul Pharmacol. 2012; 56(5-6):245-51.
18. Shen C, Beroukhim R, Schumacher SE, et al. Genetic and functional studies implicate HIF1α as a 14q kidney cancer suppressor gene. Cancer Discov. 2011; 1(3):222-35,
19. Ratcliffe PJ. HIF-1 and HIF-2: working alone or together in hypoxia? J Clin Invest. 2007; 117(4):862-865.
20. Chen W, Hill H, Christie A et al. Targeting renal cell carcinoma with a HIF-2 antagonist. Nature. 2016; 539(7627):112-1.
21. Bailey ST, Smith AM, Kardos J, et al. MYC activation cooperates with Vhl and Ink4a/Arf loss to induce clear cell renal cell carcinoma. Nat. Commun. 2017; (8): 15770.
22. Raval RR, Lau KW, Tran MG, et al. Contrasting properties of hypoxia-inducible factor 1 (HIF-1) and HIF-2 in von Hippel-Lindau-associated renal cell carcinoma. Mol. Cell. Biol. 2015; (25):5675–5686.
23. Shi J, Wang K, Xiong Z, et al. Impact of inflammation and immunotherapy in renal cell carcinoma. Oncol Lett. 2020; 20(5):272.
24. Anker J, Miller J, Taylor N et al. From Bench to Bedside: How the Tumor Microenvironment Is Impacting the Future of Immunotherapy for Renal Cell Carcinoma. Cells. 2021; 10(11):3231.
25. Vuong L, Kotecha RR, Voss MH, et al. Tumor Microenvironment Dynamics in Clear-Cell Renal Cell Carcinoma. Cancer Discov. 2019; 9(10):1349-1357.

26. Diaz de Leon A, Pirasteh A, Costa DN, et al. Current Challenges in Diagnosis and Assessment of the Response of Locally Advanced and Metastatic Renal Cell Carcinoma. Radiographics. 2019; 39(4):998-1016.
27. Bottazzi B, Inforzato A, Messa M, et al. The pentraxins PTX3 and SAP in innate immunity, regulation of inflammation and tissue remodelling. J Hepatol. 2016; 64(6):1416-27.
28. Wang Z, Wang X, Zou H, et al. The Basic Characteristics of the Pentraxin Family and Their Functions in Tumor Progression. Front Immunol. 2020; 11:1-16.
29. Doni A, Stravalaci M, Inforzato A, et al. The long pentraxin PTX3 as a link between innate immunity, tissue remodeling, and cancer. Front Immunol. 2019; 10:1-13.
30. Inforzato A, Bottazzi B, Garlanda C, et al. Pentraxins in humoral innate immunity. Adv Exp Med Biol. 2012; 946:1–20.
31. Inforzato A, Reading PC, Barbati E, et al. The “sweet” side of a long pentraxin: how glycosylation affects PTX3 functions in innate immunity and inflammation. Front Immunol. 2013; 3:407.
32. Jaillon S, Peri G, Delneste Y, et al. The humoral pattern recognition receptor PTX3 is stored in neutrophil granules and localizes in extracellular traps. J Exp Med. 2007; 204:793-804.
33. Magrini E, Mantovani A, Garlanda C, et al. The Dual Complexity of PTX3 in Health and Disease: A Balancing Act? Trends Mol Med. 2016; 22:497-510.
34. Liu S, Qu X, Liu F, et al. Pentraxin 3 as a Prognostic Biomarker in Patients with Systemic Inflammation or Infection. Mediators Inflamm. 2014; 2014:421429.
35. Bastrup-Birk S, Skjoedt MO, Munthe-Fog L, et al. Pentraxin-3 Serum Levels Are Associated with Disease Severity and Mortality in Patients with Systemic Inflammatory Response Syndrome. PLoS One 2013; 8: e73119.
36. Moalli F, Jaillon S, Inforzato A, et al. Pathogen Recognition by the Long Pentraxin PTX3. J Biomed Biotechnol 2011:830421.

37. Giacomini A, Ghedini GC, Presta M, et al. Long pentraxin 3: A novel mult, ifaceted player in cancer. Biochim Biophys Acta Rev Cancer. 2018 1869:53–63.
38. Di Virgilio F A commentary on "PTX3 is an extrinsic oncosuppressor regulatingomplement-dependent inflammation in cancer". Front Oncol. 2015; 5:118.
39. Korniluk A, Koper O, Kemona H, et al. From inflammation to cancer. Review Ir J Med Sci. 2017; 186:57-62.
40. Chang WC,Wu SL, Huang WC, et al. PTX3 gene activation in EGF-induced head and neck cancer cell metastasis. Oncotarget 2015; 6:7741-7757.
41. Chan SH, Tsai JP, Shen CJ, et al. Oleate-induced PTX3 promotes head and neck squamous cell carcinoma, metastasis through the up-regulation of vimentin. Oncotarget. 2017; 8:41364-41378.
42. Song T, Wang C, Guo C, et al. Pentraxin 3 overexpression accelerated tumor metastasis and indicated poor prognosis in hepatocellular carcinoma via driving epithelial-mesenchymal transition. J Cancer. 2018; 9:2650-2658.
43. Thomas C, Henry W, Cuiffo BG, et al. Pentraxin-3 is a PI3K signaling target that promotes stem cell-like traits in basal-like breast cancers. Sci Signal 2017; 10:eaah4674.
44. B. Choi, Lee EJ, Shin MK, et al. Upregulation of brain-derived neurotrophic factor in advanced gastric cancer contributes to bone metastatic ostolysis by inducing long pentraxin 3. Oncotarget. 2016; 7:55506-55517.
45. Rathore M, Girard C, Ohanna M, et al. Cancer cell-derived long pentraxin 3 (PTX3) promotes melanoma migration through a toll-like receptor 4 (TLR4)/NF-κB signaling pathway. Oncogene. 2019; 38:5873-5889.
46. Garlanda C, Bottazzi B, Magrini E, et al. PTX3, a humoral pattern recognition molecule, in innate immunity, tissue repair, and cancer. Physiol Rev. 2018; 98:623-639.

47. Schmid MC, Varner JA. Myeloid cell trafficking and tumor angiogenesis. Cancer Lett. 2007; 250:1-8.
48. Schröder FH, Hugosson J, Roobol MJ, et al. Screening and prostate-cancer mortality in a randomized European study. N Engl J Med. 2009; 360:1320–1328.
49. Ronca R, Giacomini A, Di Salle E, et al. Long-Pentraxine 3 derivative as a small-molecule FGF trap for cancer therapy. Cancer Cell. 2015; 28:225-239.
50. Ma YJ and Garred P. Pentraxins in Complement Activation and Regulation. Front. Immunol. 2018; 9:3046.
51. Daigo K, Hamakubo T. Host-protective effect of circulating pentraxin 3 (PTX3) and complex formation with neutrophil extracellular traps. Front Immunol. 2019; 3:378.
52. Daigo K, Inforzato A, Barajon I, et al. Pentraxins in the activation and regulation of innate immunity. Immunol. Rev 2016; 274: 202–217.
53. Braunschweig A, Jo´zsi M. Human Pentraxin 3 Binds to the Complement Regulator C4b-Binding Protein. PLoS ONE 2011; 6:e23991.
54. Revel M, Daugan MV, Sautés-Fridman C, et al. Complement System: Promoter or Suppressor of Cancer Progression? Antibodies (Basel). 2020; 9:57.
55. Rutkowski MJ, Sughrue ME, Kane AJ, et al. Cancer and the Complement Cascade. Mol Cancer Res. 2010; 8:1453–65.
56. Venkatesha RT, Thangam EB, Zaidi AK, Ali H. Distinct regulation of C3a-induced MCP-1/CCL2 and RANTES/CCL5 production in human mast cells by extracellular signal regulated kinase and PI3 kinase. Mol Immunol. 2005; 42(5):581-7.
57. Markiewski MM, DeAngelis RA, Strey CW, et al. The regulation of liver cell survival by complement. J Immunol. 2009; 182(9):5412-8.
58. Vivanco I, Sawyers CL. (2002) The phosphatidylinositol 3-kinase-AKT pathway in human cancer. Nat Rev Cancer 2(7):489-501.

59. Netti GS, Franzin R, Stasi A, Spadaccino F, et al. Role of Complement in Regulating Inflammation Processes in Renal and Prostate Cancers. Cells. 2021; 10(9):2426.
60. Stallone G, Cormio L, Netti GS, et al. Pentraxin 3: a novel biomarker for predicting progression from prostatic inflammation to prostate cancer. Cancer Res. 2014; 74(16):4230-8.
61. Manning ML, Williams SA, Jelinek CA, et al. Proteolysis of complement factors iC3b and C5 by the serine protease prostate-specific antigen in prostatic fluid and seminal plasma. J Immunol. 2013; 190:2567–2574.
62. Loberg RD, Day LL, Dunn R, Kalikin LM, et al. Inhibition of decay-accelerating factor (CD55) attenuates prostate cancer growth and survival in vivo. Neoplasia. 2006; 8:69–78.
63. Xu C, Jung M, Burkhardt M, Stephan C, et al. Increased CD59 protein expression predicts a PSA relapse in patients after radical prostatectomy. Prostate. 2015; 62:224–232.
64. Stallone G, Netti GS, Cormio L, et al. Modulation of complement activation by pentraxin-3 in prostate cancer. Sci Rep. 2020; 10(1):18400.
65. Reese B, Silwal A, Daugherity E, et al. Complement as Prognostic Biomarker and Potential Therapeutic Target in Renal Cell Carcinoma. J Immunol. 2020; 205;3218–3229.
66. Tang S, Zhou W, Sheerin NS, et al. Contribution of renal secreted complement C3 to the circulating pool in humans. J Immunol. 1999; 162:4336–4341.
67. Zhou W, Marsh JE, Sacks SH. Intrarenal synthesis of complement. Kidney Int. 2001; 59;1227–1235.
68. Corrales L, Ajona D, Rafail S, et al. Anaphylatoxin C5a creates a favorable microenvironment for lung cancer progression. J Immunol. 2012; 189;4674–4683.
69. Hezmee MNM, Kyaw-Tanner M, Lee JYP, et al. Increased expression of C5a receptor (CD88) mRNA in canine mammary tumors. Vet Immunol Immunopathol 2011; 139;50–56

70. Blok VT, Daha MR, Tijsma OM, et al. A possible role of CD46 for the protection in vivo of human renal tumor cells from complement-mediated damage. Lab Investig. 2000; 80;335–344.
71. Netti GS, Lucarelli G, Spadaccino F, et al. PTX3 modulates the immunoflogosis in tumor microenvironment and is a prognostic factor for patients with clear cell renal cell carcinoma Aging (Albany NY). 2020; 12(8): 7585–7602.
72. Lima RT, Busacca S, Almeida GM, et al. MicroRNA regulation of core apoptosis pathways in cancer. Eur J Cancer. 2011; 47(2):163–74.
73. Lee Y, Ahn C, Han J, et al. The nuclear RNase III Drosha initiates microRNA processing. Nat. Cell Biol. 2003; 425:415–419.
74. Winter J, Jung S, Keller S et al. Many roads to maturity: microRNA biogenesis pathways and their regulation. Nat Cell Biol 2009; 11:228–234.
75. Chen X, Ba Y, Ma L, et al. Characterization of microRNAs in serum: a novel class of biomarkers for diagnosis of cancer and other diseases. Cell Res. 2008; 18(10):997–1006.
76. Krol J, Sobczak K, Wilczynska U, et al. Structural features of microRNA (miRNA) precursors and their relevance to miRNA biogenesis and small interfering RNA/short hairpin RNA design. J Biol Chem. 2004; 2004:42230–9.
77. Griffiths-Jones S, Hui JHL, Marco A, et al. MicroRNA evolution by arm switching. EMBO Rep. 2011; 12:172–177.
78. Sayed D, Abdellatif M. MicroRNAs in development and disease. Physiol Rev 2011; 91(3):827–87.
79. Zhang L; Liao Y, Tang L. MicroRNA-34 family: A potential tumor suppressor and therapeutic candidate in cancer. J. Exp. Clin.Cancer Res. 2019; 38:1–13.
80. Acunzo M, Croce CM. Downregulation of miR-15a and miR-16-1 at 13q14 in Chronic Lymphocytic Leukemia. Clin. Chem. 2016; 62: 655–656.

81. Torrisani J, Parmentier L, Buscail L, et al. Enjoy the Silence: The Story of let-7 MicroRNA and Cancer. Curr. Genom. 2007; 8: 229–233.
82. Valera VA, Walter BA, Linehan WM, et al. Regulatory effects of microRNA-92 on VHL gene expression and the hypoxic activation of miR-210 in Clear Cell Renal Carcinoma. J Cancer. 2011; 2:515-26. .
83. Wang X, Chen X, Wang R, et al. microRNA-200c modulates the epithelial-to-mesenchymal transition in human renal cell carcinomametastasis. Oncol Rep. 2013; 30(2): 643-50.
84. Yoshino H, Enokida H, Itesako T et al. Epitelial-mesenchymal transition-related microRNA-200s regulate molecular targets and pathways in renal cell carcinoma. J Hum Genet. 2013; 58(8): 508-16. .
85. Spadaccino F, Gigante M, Netti GS, et al. The Ambivalent Role of miRNAs in Carcinogenesis: Involvement in Renal Cell Carcinoma and Their Clinical Applications. Pharmaceuticals 2021; 14: 322.
86. Campisi J. Aging cellular senescence, and cancer. Annu Rev Physiol. 2013; (75):685-705.
87. Mohamad Kamal NS, Safuan S et al. Aging of the cells: Insight into cellular senescence and detection Methods.Eur J Cell Biol. 2020; 99(6):151108.
88. Collado M, Blasco MA et al. Cellular senescence in cancer and aging. Cell. 2007; 130(2):223-33.
89. Childs BG, Baker DJ et al. Senescence and apoptosis: dueling or complementary cell fates? EMBO Rep. 2014; 15(11):1139-53.
90. Lee BY, Han JA et al. Senescence-associated beta-galactosidase is lysosomal beta-galactosidase. Aging Cell. 2006; 5(2):187-95.
91. Di Micco R., Fumagalli M. et al. Oncogene-induced senescence is a DNA damage response triggered by DNA hyper-replication. Nature. 2006; (444):638–642.
92. Herranz, Nicolás, and Jesús Gil. Mechanisms and functions of cellular senescence. J. Clin. Investig. 2018; (4):1238-1246.
93. Sacco A, Belloni L et al. From Development to Aging: The Path to Cellular Senescence. Antioxid Redox Signal. 2021; 34(4):294-307.

94. Bartkova J, Rezaei N et al. Oncogene-induced senescence is part of the tumorigenesis barrier imposed by DNA damage checkpoints. Nature. 2006 Nov 30; 444(7119):633-7.
95. Kumari R, Jat P. Mechanisms of Cellular Senescence: Cell Cycle Arrest and Senescence Associated Secretory Phenotype. Front Cell Dev Biol. 2021; (9):645593.
96. Coppé JP, Patil CK et al. Senescence-associated secretory phenotypes reveal cell-nonautonomous functions of oncogenic RAS and the p53 tumor suppressor. PLoS Biol. 2008; 6(12):2853-68.
97. Lopes-Paciencia S, Saint-Germain E et al. The senescence-associated secretory phenotype and its regulation. Cytokine. 2019; (117):15-22.
98. Stow JL, Murray RZ. Intracellular trafficking and secretion of inflammatory cytokines. Cytokine Growth Factor Rev. 2013; 24(3):227-39.
99. Birch J, Gil J. Senescence and the SASP: many therapeutic avenues. Genes Dev. 2020 ;34(23-24):1565-1576.
100. Weinberg RA. The retinoblastoma protein and cell cycle control. Cell. 1995; (81):323–330.
101. Henley SA, Dick FA. The retinoblastoma family of proteins and their regulatory functions in the mammalian cell division cycle. Cell Div. 2012; (7):10.
102. Chen HZ, Tsai SY et al. Emerging roles of E2Fs in cancer: an exit from cell cycle control. Nature Rev. Cancer. 2009; (9):785–797.
103. Michieli P., Chedid M et al. Induction of WAF1/CIP1 by a p53-independent pathway. Cancer Res. 1994; (54):3391–3395.
104. Giono LE, Manfredi JJ. The p53 tumor suppressor participates in multiple cell cycle checkpoints. J Cell Physiol. 2006; 209(1):13–20.
105. Baker D, Wijshake T, Tchkonia T, et al. Clearance of p16Ink4a-positive senescent cells delays ageing-associated disorders. Nature 2011; (479):232–236.
106. Gatter KC. Handbook of immunohistochemistry and in situ hybridisation of human carcinomas: molecular genetics – lung and breast carcinomas. Br J Cancer. 2005; 93(11):1318.

107. Mikuła-Pietrasik J., Niklas A. et al. Mechanisms and significance of therapy-induced and spontaneous senescence of cancer cells. Cell. Mol. Life Sci. 2020; (77):213–229.
108. Dörr JR, Yu Y, Milanovic M et al. Synthetic lethal metabolic targeting of cellular senescence in cancer therapy. Nature. 2013; 501(7467):421-5.
109. Kuilman T, Michaloglou C et al. The essence of senescence. Genes Dev. 2010; 24(22):2463-79.
110. Burton DG, Krizhanovsky et al. Physiological and pathological consequences of cellular senescence. Cell Mol Life Sci. 2014 Nov; 71(22):4373-86.
111. Birch J, Gil J. Senescence and the SASP: many therapeutic avenues. Genes Dev. 2020; 34(23-24):1565-1576.
112. Coppe JP, Patil CK, Rodier F, et al. Senescence-associated secretory phenotypes reveal cell-nonautonomous functions of oncogenic RAS and the p53 tumor suppressor. PLoS Biology. 2008; 6(12), 2853–2868.
113. Kuilman, T, Michaloglou C, Vredeveld LC, et al. Oncogene-induced senescence relayed by an interleukin-dependent inflammatory network. Cell. 2008; 133, 1019–1031.
114. Garfinkel S, Brown S, Wessendorf JH, Maciag T. Post-transcriptional regulation of interleukin 1 alpha in various strains of young and senescent human umbilical vein endothelial cells. Proc Natl Acad Sci U S A. 1994; 91(4), 1559–1563.
115. Ritschka B, Storer M, Mas A et al. The senescence-associated secretory phenotype induces cellular plasticity and tissue regeneration. Genes Dev. 2017; 31(2):172-183.
116. Coppé JP, Patil CK, Rodier F, et al. Senescence-associated secretory phenotypes reveal cell-nonautonomous functions of oncogenic RAS and the p53 tumor suppressor. PLoS Biol. 2008; 6: 2853– 68.
117. Canino C, Mori F, Cambria A, et al. SASP mediates chemoresistance and tumor-initiating-activity of mesothelioma cells. Oncogene. 2012; 31: 3148– 63.

118. Bavik C, Coleman I, Dean JP, et al. The gene expression program of prostate fibroblast senescence modulates neoplastic epithelial cell proliferation through paracrine mechanisms. Cancer Res. 2006; 66: 794– 802.
119. Coppé JP, Kauser K, Campisi J, et al. Secretion of vascular endothelial growth factor by primary human fibroblasts at senescence. J Biol Chem. 2006; 281: 29568– 74.
120. Liu, D., & Hornsby, P. J. Senescent human fibroblasts increase the early growth of xenograft tumors via matrix metalloproteinase secretion. Cancer Res. 2007; 67, 3117–3126.
121. West MD, Pereira-Smith OM, Smith, JR. Replicative senescence of human skin fibroblasts correlates with a loss of regulation and overexpression of collagenase activity. Experimental Cell Res. 1989; 184, 138–147.
122. McQuibban GA, Gong JH, Wong JP, et al. Matrix metalloproteinase processing of monocyte chemoattractant proteins generates CC chemokine receptor antagonists with anti-inflammatory properties in vivo. Blood. 2002; 100(4), 1160–1167.
123. Finkel T, Holbrook NJ. Oxidants, oxidative stress and the biology of ageing. Nature. 2000; 408, 239–247.
124. Costa J, Casimiro S, Pacheco T, et al. Therapy-induced cellular senescence induces epithelial-to-mesenchymal transition and increases invasiveness in rectal cancer. Clin Colorectal Cancer. 2016; 15: 170– 178.
125. Acosta JC, Banito A, Wuestefeld T, et al. A complex secretory program orchestrated by the inflammasome controls paracrine senescence. Nat Cell Biol. 2013; 15: 978– 90.
126. Mosteiro L, Pantoja C, Alcazar N, et al. Tissue damage and senescence provide critical signals for cellular reprogramming in vivo. Science. 2016; 354:aaf4445.
127. Mosteiro L, Pantoja C, de Martino A, et al. Senescence promotes in vivo reprogramming through p16(INK)(4a) and IL-6. Aging Cell. 2018; 17:e12711.

128. Takasugi M, Yoshida Y, Hara E, et al. The role of cellular senescence and SASP in tumour microenvironment. The FEBS journal. 2022.
129. Fane M, Weeraratna AT. How the Ageing Microenvironment Influences Tumour Progression. Nat Rev Cancer. 2020; 20:89–106.
130. Jonasch E, Walker CL, Rathmell WK. Clear Cell Renal Cell Carcinoma Ontogeny and Mechanisms of Lethality. Nat Rev Nephrol 2021; 17:245–61. .
131. Zhou P, Liu Z, Hu H, et al. Comprehensive Analysis of Senescence Characteristics Defines a Novel Prognostic Signature to Guide Personalized Treatment for Clear Cell Renal Cell Carcinoma. Front Immunol. 2022; 13:901671.
132. Li J, Gui C, Yao H, et al. An Aging and Senescence-Related Gene Signature for Prognosis Prediction in Clear Cell Renal Cell Carcinoma. Front Genet. 2022; 13:871088.
133. Schmitt R, Melk A. Molecular mechanisms of renal aging. Kidney Int. 2017 Sep;92(3):569-579.
134. Oishi H, Doi S, Nakashima A, et al. Klotho overexpression protects against renal aging along with suppression of transforming growth factor-β1 signaling pathways. Am J Physiol Renal Physiol. 2021; 321(6):F799-F811.
135. Che R, Yuan Y, Huang S, et al. Mitochondrial dysfunction in the pathophysiology of renal diseases. Am J Physiol Renal Physiol. 2014; 306(4):F367-78.
136. Yang H, Fogo AB. Cell senescence in the aging kidney. J Am Soc Nephrol. 2010; 21(9):1436-9.
137. Demaria M, O'Leary MN, Chang J, et al. Cellular Senescence Promotes Adverse Effects of Chemotherapy and Cancer Relapse. Cancer Discov. 2017; 7(2):165-176. .
138. Hernandez-Segura A, Nehme J, Demaria M. Hallmarks of Cellular Senescence. Trends Cell Biol. 2018; 28(6):436-453. .
139. Franzin R, Stasi A, Ranieri E, et al. Targeting Premature Renal Aging: from Molecular Mechanisms of Cellular Senescence to Senolytic Trials. Front Pharmacol. 2021; 12:630419.

140. Zhang L, Huang L, Chen G, et al. Potential Targets and Clinical Value of MiR-224-5p in Cancers of the Digestive Tract Cell PhysiolBiochem 2017; 44:682–700.
141. He X, Zhang Z, Li M, et al. Expression and role of oncogenic miRNA-224 in esophageal squamous cell carcinoma. BMC Cancer. 2015; 15:575.
142. Cui R, Meng W, Sun HL, et al. MicroRNA-224 promotes tumor progression in nonsmall cell lung cancer. ProcNatlAcad Sci U S A. 2015; 112: E4288–E4297.
143. Wang M, Deng X, Ying Q, et al. MicroRNA-224 targets ERG2 and contributes to malignant progressions of meningioma. BiochemBiophys Res Commun. 2015; 460:354–361.
144. Zhiyuan Q, HaihongH,Wen S, et al. miR-224-5p Contained in Urinary Extracellular Vesicles Regulates PD-L1 Expression by Inhibiting Cyclin D1 in Renal Cell Carcinoma Cells. Cancers 2021; 13(4):618.
145. Yifei L, Honglin N, Yubo Z, et al. MiR-224-5p Targeting OCLN Promotes the Proliferation, Migration, and Invasion of Clear Cell Renal Cell Carcinoma Cells. Urol Int. 2021; 1-10.
146. Hwang HW, Baxter LL, Loftus SK, et al. Distinct microRNA expression signatures are associated with melanoma subtypes and are regulated by HIF1A. Pigment Cell Melanoma Res. 2014; 27:777–787.
147. Chuan H, Libo W, Jiantao Z, et al. Hypoxia-inducible microRNA-224 promotes the cell growth, migration and invasion by directly targeting RASSF8 in gastric cancer. Mol Cancer. 2017; 16: 35.
148. Xiufang L, Huidan W, Yan S, et al. MicroRNA-224 delays oocyte maturation through targeting Ptx3 in cumulus cells. Mech Dev. 2017;143: 20-25.
149. Li-Mei Y, Wei-Wei W, Rong Q, et al. MicroRNA-224 inhibition prevents progression of cervical carcinoma by targeting PTX3. J Cell Biochem. 2018 ;119(12):10278-10290.

150. Bin-LiangG,Li-Jie Z, Li G, et al. Downregulation of miR-224-5p in prostate cancer and its relevant molecular mechanism via TCGA, GEO database and in silico analyses Oncol Rep. 2018; 40(6): 3171–3188.
151. Rudnicki A, Shivatzki S, Beyer LA, et al. microRNA-224 regulates Pentraxin 3, a component of the humoral arm of innate immunity, in inner ear inflammation. Hum Mol Genet. 2014; 23(12): 3138–3146.
152. O'Brien J, Hayder H, Zayed Y, et al. Overview of MicroRNA Biogenesis, Mechanisms of Actions, and Circulation Front. Endocrinol. 2018; 9:402.
153. Min X, Jin L, Wei L, et al. MicroRNAs activate gene transcription epigenetically as an enhancer trigger. RNA Biol. 2017; 14(10): 1326–1334.
154. Ramchandran R, Chaluvally-Raghavan P. miRNA-Mediated RNA Activation in Mammalian Cells. AdvExp Med Biol. 2017; 983:81-89.
155. Gu Y, Guo Y, Gao N. et al. The proteomic characterization of the peritumor microenvironment in human hepatocellular carcinoma. Oncogene. 2022;41: 2480–2491.
156. Huang C, Liu H, Gong X, et al. Analysis of different components in the peritumoral tissue microenvironment of colorectal cancer: A potential prospect in tumorigenesis. Mol Med Rep. 2016; 14(3):2555-65.
157. Zhang S, Yang X, Wang L et al. Interplay between inflammatory tumor microenvironment and cancer stem cells (Review). Oncol Lett. 2018; 16: 679-686.
158. Jang JH, Kim DH, Surh, YJ. Dynamic roles of inflammasomes in inflammatory tumor microenvironment. npj Precis. Onc. 2021; 5, 18. 2021.
159. Wiley CD, Campisi J. From Ancient Pathways to Aging Cells-Connecting Metabolism and Cellular Senescence. Cell Metab. 2016; 14;23(6):1013-1021.

160. Shariat SF, Tokunaga H, Zhou J, et al. p53, p21, pRB, and p16 expression predict clinical outcome in cystectomy with bladder cancer. J Clin Oncol. 2004; 22(6):1014-24.
161. Ueki K, Ono Y, Henson JW, et al. CDKN2/p16 or RB alterations occur in the majority of glioblastomas and are inversely correlated. Cancer Res 1996; 56: 150–153.
162. Serrano M. The tumor suppressor protein p16INK4a. Exp Cell Res 1997; 237: 7–13.
163. Bardeesy N, Aguirre AJ, Chu GC, et al. Both p16(Ink4a) and the p19(Arf)-p53 pathway constrain progression of pancreatic adenocarcinoma in the mouse. Proc Natl Acad Sci USA 2006; 103: 5947–5952.
164. Chao DL, Sanchez CA, Galipeau PC, et al. Cell proliferation, cell cycle abnormalities, and cancer outcome in patients with Barrett's esophagus: a long-term prospective study. Clin Cancer Res 2008; 14: 6988–6995.
165. Weiss RH, Borowsky AD, Seligson D, et al p21 is a prognostic marker for renal cell carcinoma: implications for novel therapeutic approaches. J Urol. 2007; 177(1):63-8.
166. Ikuerowo SO, Kuczyk MA, von Wasielewski R. p16INK4a Expression and Clinicopathologic Parameters in Renal Cell Carcinoma Kidney Cancer 2007; 51, 3: p732-738.
167. Buj R, Chen CW, Dahl ES, et al. Suppression of p16 induces mTORC1-mediated nucleotide metabolic reprogramming. Cell Rep. 2019; 28:1971–80.
168. Liu JY, Souroullas GP, Diekman BO, et al. Cells exhibiting strong p16INK4a promoter activation in vivo display features of senescence. Proc Natl Acad Sci USA. 2019; 116:2603–11. .
169. Rodier F, Coppé JP, Patil CK, et al. Persistent DNA damage signalling triggers senescence-associated inflammatory cytokine secretion. Nat Cell Biol. 2009; 11:973–79. .

170. Meyer P, Maity P, Burkovski A, et al. A model of the onset of the senescence associated secretory phenotype after DNA damage induced senescence. PLoS Comput Biol. 2017; 13:e1005741. .
171. Buj R, Leon KE, Anguelov MA, et al. Suppression of p16 alleviates the senescence-associated secretory phenotype. Aging (Albany NY). 2021; 13(3):3290-3312. .
172. Al-Ansari MM, Aboussekhra A. miR-146b-5p mediates p16-dependent repression of IL-6 and suppresses paracrine procarcinogenic effects of breast stromal fibroblasts. Oncotarget. 2015; 6(30):30006-16.
173. Mosteiro L, Pantoja C, de Martino A, et al. Senescence promotes in vivo reprogramming through p16INK4a and IL-6. Aging Cell. 2018; 17(2):e12711. .
174. Tsukamoto T, Kumamoto Y, Miyao N, et al. Interleukin-6 in Renal Cell Carcinoma. J Urol. 1992; 148:1778–1781.
175. Blay J-Y, Rossi J-F, Wijdenes J, et al. Role of interleukin-6 in the paraneoplastic inflammatory syndrome associated with renal-cell carcinoma. Int J Cancer. 1997; 72:424–430.
176. Ishibashi K, Koguchi T, Matsuoka K, et al. Interleukin-6 induces drug resistance in renal cell carcinoma. Fukushima J Med Sci. 2018; 64(3):103-110.
177. Visconti VV, Greggi C, Fittipaldi S, et al. The long pentraxin PTX3: a novel serum marker to improve the prediction of osteoporosis and osteoarthritis bone-related phenotypes. J Orthop Surg Res. 2021; 16: 288.
178. Slusher AL, Zúñiga TM, Acevedo EO. Inflamm-Aging Is Associated with Lower Plasma PTX3 Concentrations and an Impaired Capacity of PBMCs to Express hTERT following LPS Stimulation. Mediators Inflamm. 2019; 2019: 2324193.
179. Tung JN, Ko CP, Yang SF, et al. Inhibition of pentraxin 3 in glioma cells impairs proliferation and invasion in vitro and in vivo. J Neurooncol. 2016; 129(2):201-9.
180. Mier, James W. “The tumor microenvironment in renal cell cancer.” Curr Opin Oncol. 2019; 31(3):194-199.